



# Analytical framework for real-gas mixtures with phase-equilibrium thermodynamics

P. Tudisco\*, S. Menon

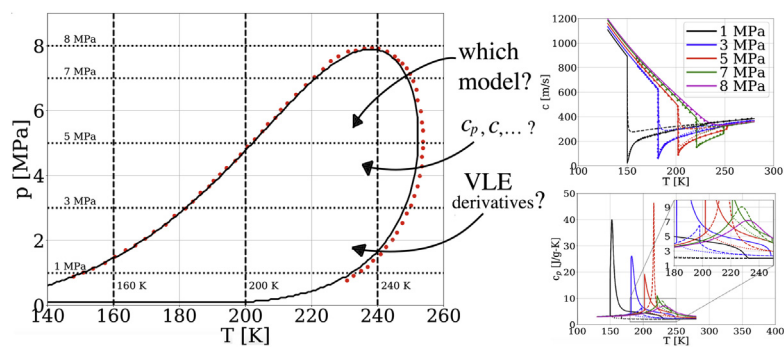
School of Aerospace Engineering, Georgia Institute of Technology, 270 First Drive, Atlanta, GA 30332, USA



## HIGHLIGHTS

- Found novel analytical representation of mixture thermodynamic properties with phase equilibrium.
- Verified importance of this fully analytical, thermodynamically consistent model against pre-existing approaches.
- Some phase-related thermodynamic derivatives cannot be neglected.
- Proven the superior computational speed of the present method against the previously used fully numerical approaches.

## GRAPHICAL ABSTRACT



## ARTICLE INFO

### Article history:

Received 19 March 2020

Received in revised form 15 May 2020

Accepted 3 June 2020

Available online 18 June 2020

### Keywords:

Super-critical mixing  
Vapor-liquid equilibrium  
Thermodynamic properties  
Generic equation of state

## ABSTRACT

Real-gas (RG) thermodynamics is currently being employed in many fields of science and engineering ranging from energy production to planetary exploration to combustion and fluid mechanics. Particularly prediction of phase equilibrium, *i.e.* the condition at which two or more phases occur simultaneously in a multi-component mixture is of key importance because it represents a thermodynamic state that is more stable given that it occurs at a lower value of Gibbs free energy compared to the corresponding single phase state (*i.e.* only one phase exists). While the calculation of phase-equilibrium is a well-established tool, the determination of all the thermodynamic variables in the multi-phase mixture is relatively new and unexplored. In this work, we provide the complete analytical framework to compute multi-phase (we focus only on two phases for now), equilibrium properties in a generic multi-component system and demonstrate on mixtures with increasing level of complexity that approximate methods, sometimes used in the literature, provide inaccurate predictions, thus making the present model an important framework for all the simulation tools that employ RG thermodynamics with phase-equilibrium.

© 2020 Elsevier B.V. All rights reserved.

## 1. Introduction

Real-gas (RG) thermodynamics is typically employed to model complex systems at conditions that are far from ideal, meaning that they cannot be represented by simply using the common ideal-gas (IG) equation of state (EoS). Qualitatively an IG mixture is defined as such, when its density is relatively "low", which is commonly achieved when its thermodynamic state involves low pressures and high

\* Corresponding author.

E-mail address: [ptudisco3@gatech.edu](mailto:ptudisco3@gatech.edu) (P. Tudisco).

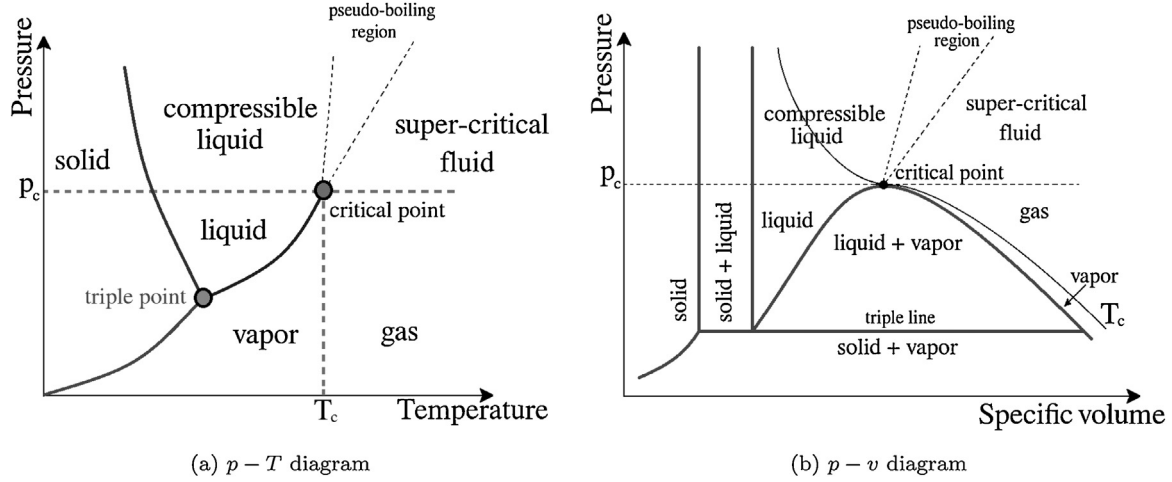


**Fig. 1.** Schematics of (a) pressure-temperature and (b) pressure-specific volume diagram for a generic single component.

temperatures. More rigorously, an IG mixture can be defined only when its compressibility is equal to one, which is often violated in engineering and scientific applications.

Evidence of this fact can be found in many published works, ranging from the CO<sub>2</sub> processing [1–3], to heat exchangers design and cooling [4–8], to Earth and planetary exploration [9,10], to fluid mechanics and combustion applications [11–17]. Particularly in our recent work [17], we began to study the problem of multi-component mixing at super-critical conditions with the ultimate goal to apply it to practical engine configuration as done in past using the IG EoS [18,19]. We faced the challenge to couple a fully compressible, multi-species solver with a thermodynamically consistent mixing model involving phase-equilibrium and a stable numerical scheme to handle the high-density gradients. In that work [17], the thermodynamic consistency of the mixing model was achieved using numerical derivatives as suggested by [20], however in this work we provide the corresponding fully analytical model (not present in the literature in the current form to the authors' knowledge), which overall increases performance and accuracy compared to the numerical approach.

While the IG EoS is by definition capable to predict gaseous phases only, more sophisticated EoS to study RG mixtures with phase-equilibrium need to have the capability to predict at least two phases, for instance the liquid and the gaseous ones, which are going to be the focus of this work. As a result, for a single component, the *critical point* given by the values of the species-dependent critical pressure  $p_c$  and critical temperature  $T_c$ , represents one threshold between different physical states, which can be further divided into sub-categories, as depicted in Fig. 1. In order to introduce to the problem of RG mixtures with phase equilibrium, consider first Fig. 1(a), which refers to the  $p-T$  diagram of a single species. The generic substance may experience variation in its phase as its thermodynamic state is modified. However some transitions are *sharp* while other transitions are *smooth* [21,22]. For example, the transition between the liquid and the vapor phase is sharp and involves the exchange of some amount of energy, the *latent heat of vaporization*, to transition from one region to another: energy has to be added in the case of isothermal vaporization and energy has to be removed in the case of isothermal condensation. On the other hand, the transition between super-critical states, *i.e.* the states that occur for pressures higher than the critical value, such as from compressible liquid to super-critical fluid, exhibit a smooth transition, called “*pseudo boiling*” region, in which properties vary more regularly, without any abrupt change [23]. This means that properties specifically related to the sub-critical regime, such as the heat of vaporization and even surface tension are absent in the super-critical regime as pointed out by a number of experimental works [24–36].

These observations motivated the modeling of RG mixtures at super-critical conditions using a single EoS (particularly in the field of fluid mechanics [12,13,37–50]) without the need to adopt any additional interfacial model between the compressible liquid and the super-critical fluid due to the absence of a real interface [51,52]. This also translates into the concept of *single fluid* approach to indicate the use of a single EoS in the pure super-critical region.

However, this approach relies on the fact that for some (undefined) high-pressure threshold, the mixture forms one phase at most, even in the case of multi-component. While local multi-phase conditions can occur as pointed out in many chemical engineering applications (see [22,53–56] and references therein), as well as recent works in the field of fluid-mechanics [16,17,57–60]. This immediately establishes the importance to consider multi-phase (*i.e.* more than one phase concurrently), versus single-phase conditions in RG thermodynamics.

Dealing with *phase equilibrium* [61,62] thermodynamics means to have the capability to predict at least two phases, therefore adequate EoS models have to be chosen. In addition, multi-component systems require specific care because the critical point is also a function of the mixture composition itself and additionally, setting the mixture thermodynamic state, say pressure and temperature, at a value that ensures each component to be separately super-critical (if each was taken alone), does not ensure the mixture to be in a super-critical state [22,63]. More specifically, the mixture can still form local vapor-liquid equilibrium (VLE) domes, where the EoS alone would fail to predict the correct thermodynamic state with errors that can vary depending on the state and the mixture itself as showed in this work. The reason is related to the fact that in presence of VLE, additional thermodynamic variables, such as a *phase fraction* must be taken into account according to thermodynamic laws.

Failure to do so may produce robustness reduction of the numerical tools used to solve any thermodynamic problem, for instance the calculation of pressure and temperature out of internal energy and density. Forcing the solution to behave as a “*single-fluid*” in a region where effectively phase equilibrium naturally occurs can cause erroneous values of the results or convergence issues in the iterative procedure as discussed in [17].

While algorithms to detect phase-equilibrium are well established [54,61,62] and continuously updated for robustness, convergence and range of application [53,64–67], less attention is devoted to the calculation of all other thermodynamic mixture properties in presence of VLE that are used in simulations tools. One example is the work of [86] who reported the use of VLE with highly accurate EoS such

as Helmholtz. In this work, the VLE problem is addressed and the importance of the accuracy embedded with the EoS is provided as well, however VLE thermodynamic properties are not discussed. Other works instead [87,88] tackle the issue by providing good amount of thermodynamic relationships [87] and by expressing the derivatives of the VLE by exploiting their dependency on specific volume and enthalpy. However how to actually compute these quantities is not provided for multi-component mixtures and in fact it is later showed only for single-component systems [88]. Due to the fact that VLE thermodynamic properties for multi-component systems are not extensively treated in the literature, this is the scope of the current work.

This point was also raised in the works of Traxinger et al. [60,68], Mattheis et al. [59]. However, these works lack the key details regarding the general thermodynamic framework of such mixtures that exhibit VLE, particularly: (a) they limit the discussion to very few thermodynamic properties, while a numerical simulation requires the whole calculation of thermodynamic variables that are used in the governing equations and (b) use of RG EoS with phase equilibrium requires the whole thermodynamic model to be adapted consistently to all variables. For example what are the specific heats in the VLE region? Or what is the derivative  $(\partial p/\partial \rho)_{T,X}$  which is crucial to compute the speed of sound? What about partial molar quantities which are necessary to compute the generalized heat flux? Some works have reported the application of a simple linear blending rule between the liquid (L) and the vapor (V) phase for the mixture specific heat at constant pressure  $c_p$  in the VLE region, computed as  $c_p = \beta c_p^V + (1 - \beta)c_p^L$  [56], where  $\beta$  indicates the mole fraction of the vapor phase in the mixture. This approach leads to significant departures from the actual solution as showed in Section 4, as well as further discussed in Appendix B. In some works the complete methodology used is not discussed, despite their use of VLE thermodynamics [59]. Other works [16,69] use an approximate formula to compute the speed of sound in the two phase region based on the method of Wood [83]. Finally, in the works of [17,60,68], the correct model based on the numerical framework proposed by [20] is used, however this model carries its own limitations, particularly related to the order of accuracy of the numerical derivatives and their associated computational cost which is discussed in this work. This lack of information, incorrect approaches or limitations of the pre-existing models motivated our further investigation of RG thermodynamics coupled with VLE.

Works of [53,70], devoted substantial efforts to the calculation of thermodynamic properties in two phase systems, however their focus is limited to some variables only, particularly the speed of sound and the compressibilities.

In this work, we overcome these limitations and provide a complete analytical framework for RG mixtures with phase-equilibrium. The derivation of the thermodynamic variables is made by using a different set of independent variables compared to those used in the works of [53,70] and we extend their formulation to incorporate more mixture, as well as phase specific quantities, currently not existent in the literature to the authors' knowledge. Furthermore, we provide a direct comparison between this analytical model with two simplified models, namely the single-fluid model in which the VLE presence is ignored upfront and the frozen VLE model, which neglects the presence of some derivatives that are shown to be of crucial importance. Results prove the fact that the simplified models can exhibit large departures from the complete model, independently of the mixture complexity and therefore provide the conclusion that the present thermodynamic model becomes important when simulations are carried out in all the fields discussed above that aim to use RG thermodynamics in presence of phase equilibrium. Finally, we also prove that the present analytical model performs better than the corresponding fully numerical approach proposed by [20] which we have already used and validated in our recent work [17].

This article is organized as follows: Section 2 introduces the notation through a review of the known single-phase RG thermodynamics, Section 3 discusses the same thermodynamic variables used in the single-phase case, now extended to the multi-phase equilibrium condition and provides their analytical derivation, which is the novel part of this work, Section 4 shows the results and discusses the importance of the present model versus pre-existing models before the conclusions provided in Section 5. Due to a considerable amount of derivations involved that are quite necessary to complete the mathematical description of the present model and given that these are not found, in this form in the literature (to the authors' knowledge), we preferred to include all the details in several appendices. These appendices are not strictly required to follow the paper main stream, however they result of particular importance when it comes to the details about the model derivation, implementation and comparison with other discussed models.

## 2. Review of single-phase, real-gas thermodynamics

In this section, we provide a review of single-phase RG thermodynamics and introduce to the symbols and indispensable definitions that are going to be useful throughout the rest of the work. Let  $p$ ,  $T$ ,  $\rho$  the pressure, the temperature and the density of a multi-component mixture with  $N_s$  species, each having mole fraction  $X_i$ , molecular weight  $MW_i$  and molar mass  $M_i = MW_i/1000$ ,  $i = 1, \dots, N_s$ . Without loss of generality, the link between the above state variables can be expressed through a general form of EoS that is explicit in pressure:

$$p = p(T, \rho, \mathbf{X}), \quad (2.1)$$

where  $\mathbf{X} = \{X_i | i = 1, \dots, N_s\}$  is the set of mole fractions. Using its definition, the compressibility factor  $Z$  is also given:

$$Z = \frac{pM}{\rho R_u T}, \quad (2.2)$$

where  $R_u = 8.31451 \text{ J/mol-K}$  is the universal gas constant,  $M = \sum_{i=1}^{N_s} M_i X_i$ , is the mixture molar mass and  $V = M/\rho$  is the mixture molar volume. In the following, partial derivatives will be in general expressed as  $(\partial(\cdot)/\partial(\circ))_x$  notation, where  $x$ , represents the variable or the set of variables that is considered constant during the derivation process and will be specified accordingly. Finally, variables denoted with over bars, such as  $\bar{\Psi}$  represent the extensive quantity corresponding to the intensive quantity  $\Psi$ . For a mole-based intensive quantity, the relationship  $\bar{\Psi} = N\Psi$  holds, where  $N = \sum_{i=1}^{N_s} N_i$  is the sum of the number of moles for each species  $N_i$  in the mixture.

Departure functions are constructed from the principle of corresponding states [22] and define the deviations that the actual real-gas property has compared to the corresponding ideal-gas value. Indicating as  $\Delta\Phi = \Phi - \Phi^{ig}$  the departure function of a generic thermodynamic, mole-based, intensive variable  $\Phi$  with respect to its corresponding ideal gas value  $\Phi^{ig}$ , the (intensive) internal energy  $E$ , enthalpy  $H$ , entropy  $S$ , Gibbs energy  $G = H - TS$  and Helmholtz energy  $A = G - pV$  departure functions  $\Delta\Phi = [\Delta E, \Delta H, \Delta S, \Delta G, \Delta A]$  are defined by maintaining  $T$ ,  $p$  and  $\mathbf{X}$  constant [22] (See Appendix C). Regarding the corresponding IG value  $\Phi^{ig}$ , the general form can be expressed as  $\Phi^{ig} = \sum_{i=1}^{N_s} X_i \psi_i^{ig}$ , where  $\psi_i^{ig}$  is the  $i$ -th species, mole-based, IG property that can be obtained, for example, using the NASA 9-coefficients

[71] or CHEMKIN 7-coefficients [72] polynomials. Note that in case of entropy,  $\psi_i^{\text{ig}}$  is also a function of pressure, therefore the result obtained from the polynomials must be added to the pressure term  $-R_u \ln(p/1\text{bar})$ . Moreover, when ideal-gas mixture entropy is computed, the additional mixing term  $-R_u \sum_{i=1}^{N_s} X_i \ln X_i$  needs to be added to  $\Phi^{\text{ig}}$  [21]. These additional terms have also an impact on the calculation of the Gibbs and Helmholtz energies according to their definitions.

Similarly, one can compute the molar specific heats departure functions  $\Delta c_v$  and  $\Delta c_p$  starting from their definition (See Appendix C). On the other hand, the isentropic speed of sound is provided by [20]:

$$c^2 = \left( \frac{\partial p}{\partial \rho} \right)_{s,\mathbf{x}} = \gamma \left( \frac{\partial p}{\partial \rho} \right)_{T,\mathbf{x}}. \quad (2.3)$$

Where  $\gamma = c_p/c_v$  is the specific heats ratio. Next, introducing the definition of the isobaric expansivity  $\alpha_p = -\frac{1}{\rho} \left( \frac{\partial \rho}{\partial T} \right)_{p,\mathbf{x}}$  and isothermal compressibility  $\kappa_T = \left[ \rho \left( \frac{\partial p}{\partial \rho} \right)_{T,\mathbf{x}} \right]^{-1}$  [21], we can define another important quantity: the isentropic compressibility  $\kappa_s$  as [63]:  $\kappa_s = \kappa_T - T \alpha_p^2 / \rho c_p$ . In this way, a different definition of the speed of sound can be obtained, which will result useful for later discussion:

$$c^2 = \frac{1}{\kappa_s \rho}. \quad (2.4)$$

Another important relationship between  $c_p$ ,  $c_v$  and  $\alpha_p$  is given by [21]:

$$c_p - c_v = \frac{T M}{\rho^2} \left( \frac{\partial p}{\partial T} \right)_{\rho,\mathbf{x}} \left( \frac{\partial \rho}{\partial T} \right)_{p,\mathbf{x}} = T \frac{M}{\rho} \frac{\alpha_p^2}{\kappa_T}. \quad (2.5)$$

At this stage, the derivatives  $(\partial p/\partial T)_{\rho,\mathbf{x}}$ ,  $(\partial \rho/\partial T)_{p,\mathbf{x}}$  and  $(\partial p/\partial \rho)_{T,\mathbf{x}}$  are assumed to be known with the analytical expression of the EoS in Eq. (2.1). Note that the definitions of  $c$ ,  $\alpha_p$ ,  $\kappa_T$ ,  $\kappa_s$  and Eq. (2.5) also hold for multi-phase mixtures, as long as all the derivatives involved are computed correctly. This means that the EoS alone is no longer enough and additional information on the phase equilibrium, and its derivatives are required. This is discussed in Section 3.2. The partial molar quantity of a generic intensive mixture property  $\Psi$  is defined for each species  $i$  as [21]:

$$\Psi_i = \left( \frac{\partial \Psi}{\partial N_i} \right)_{T,p,\mathbf{N}_i} = \left( \frac{\partial N \Psi}{\partial N_i} \right)_{T,p,\mathbf{N}_i}, \quad i = 1, \dots, N_s \quad (2.6)$$

where  $\mathbf{N}_i = \{N_j | j = 1, \dots, N_s, j \neq i\}$ . The set of partial molar quantities has the unique property to satisfy the following relationship:  $\Psi = \sum_{i=1}^{N_s} \Psi_i X_i$ . For an IG the relationship simplifies to  $\Psi_i = \psi_i^{\text{ig}}$  because  $\Psi \equiv \Phi^{\text{ig}}$  defined earlier. We are interested in the expressions of partial molar volume and partial molar enthalpy, both particularly useful for example in the determination of mass and energy diffusion terms [73]:

$$V_i = \left( \frac{\partial \bar{V}}{\partial N_i} \right)_{T,p,\mathbf{N}_i} = \left( \frac{\partial N \bar{V}}{\partial N_i} \right)_{T,p,\mathbf{N}_i}, \quad h_i = \left( \frac{\partial \bar{H}}{\partial N_i} \right)_{T,p,\mathbf{N}_i} = \left( \frac{\partial N \bar{H}}{\partial N_i} \right)_{T,p,\mathbf{N}_i}. \quad (2.7)$$

The fugacity  $f_i$  of the  $i$ th species in a non-ideal mixture is used in place of the pressure to describe RG behaviors of the species alone, as well as in the mixture. One way to introduce it is through the so-called *fugacity coefficient*  $\phi_i(T, p, \mathbf{X}) = f_i(T, p, \mathbf{X})/p X_i$  [21,22], which is available analytically with a given EoS model (See Appendix C for details).

### 3. Multi-phase equilibrium, real-gas thermodynamics

In this section, we first introduce to the known concept of VLE applied for a generic, multi-component mixture at given temperature,  $T$ , pressure  $p$  and composition  $\mathbf{X}$ . Next, we derive all the multi-phase, thermodynamic properties in presence of VLE, which constitutes a key contribution of this work.

#### 3.1. The VLE problem

To represent multi-phase behavior of multi-component mixtures, we invoke the assumption of phase equilibrium (VLE) throughout the calculations. This assumption imposes equality of pressure, temperature and fugacity of both the liquid (L) and the vapor (V) phase such that [22]:

$$p_L = p_V = p; \quad T_L = T_V = T; \quad f_i^L = f_i^V \quad i = 1, \dots, N_s. \quad (3.1)$$

Note that this method assumes two or more components in the system. For single component one can use other methods such as Clausius-Clapeyron equation discussed in classical thermodynamic books, or Maxwell's method or Antoine's equation [22]. An additional unknown  $\beta$  is introduced, which indicates the ratio between the mixture number of moles in the vapor phase over the total number of moles. Then, mass conservation imposes [53]:  $X_i = \beta y_i + (1 - \beta)x_i$ , where  $x_i$  and  $y_i$  correspond to the mole fractions of species  $i$  in the liquid and the vapor phase, respectively. Both  $x_i$  and  $y_i$  satisfy the condition:  $\sum_{i=1}^{N_s} x_i = 1$  and  $\sum_{i=1}^{N_s} y_i = 1$ . For each phase taken separately, still all the formulas discussed in Section 2 hold, provided that the substitution  $x_i \leftarrow X_i$  and  $y_i \leftarrow X_i$  is made for the liquid and the vapor phase, respectively, wherever mole fractions are used, including the calculation of the phase molar mass  $M$ .

Additional *blend rules* for the phase properties are required in order to define the properties of the whole mixture and close the problem. Two extensive properties are required to be blended. In this work, similarly to other works [55,59], we blend the extensive volume and the extensive internal energy, however other approaches are possible where volume and enthalpy are blended [57]:

$$\bar{V} = \bar{V}^V + \bar{V}^L \rightarrow NV = N^V V^V + N^L V^L \rightarrow V = \frac{M}{\rho} = \frac{N^V}{N} \frac{M^V}{\rho^V} + \frac{N^L}{N} \frac{M^L}{\rho^L}, \quad (3.2)$$

$$\bar{E} = \bar{E}^V + \bar{E}^L \rightarrow NE = N^V E^V + N^L E^L \rightarrow E = \frac{N^V}{N} E^V + \frac{N^L}{N} E^L, \quad (3.3)$$

where  $N$ ,  $N^L$  and  $N^V$  are the total number of moles of the mixture, liquid and vapor phase respectively. Therefore, by using the definition  $\beta = N^V/N$  and observing that  $N = N^L + N^V$  for continuity, the accessory state relations for the multi-phase equilibrium thermodynamics become:

$$\frac{M}{\rho} = \beta \frac{M^V}{\rho^V} + (1 - \beta) \frac{M^L}{\rho^L} \quad (3.4)$$

$$E = \beta E^V + (1 - \beta) E^L. \quad (3.5)$$

In the above, for example the vapor molar mass  $M^V = M^V(\mathbf{y})$  and the vapor phase internal energy is  $E^V = E^V(T, p, \mathbf{y})$ , with  $\mathbf{y} = \{y_i | i = 1, \dots, N_s\}$ . Both can be computed using the single phase thermodynamics formulas, however  $\mathbf{y}$  is unknown and needs to be computed along with  $\mathbf{x} = \{x_i | i = 1, \dots, N_s\}$  and  $\beta$ . Also note that Eqs. (3.4) and (3.5) naturally collapse into the single phase identities in case a pure liquid ( $\beta = 0$ ,  $\mathbf{x} = \mathbf{X}$ ) or a pure vapor ( $\beta = 1$ ,  $\mathbf{y} = \mathbf{X}$ ) exist. The latter conditions may happen either in a sub-critical (pure liquid or pure gas/vapor) or super-critical (compressible liquid or super-critical fluid) state, similarly to what depicted in Fig. 1(a) and (b) for a single component.

To find the unknowns, the fugacity equalities of Eq. (3.1) are recast in form of fugacity coefficient and defining the vapor to liquid phase mole fractions ratio for each  $i$ th component  $K_i = y_i/x_i$  one obtains a set of  $N_s$  non linear algebraic equations, to which an additional constraint  $\sum_{i=1}^{N_s} x_i - \sum_{i=1}^{N_s} y_i = 0$  needs to be added. This latter constraint can be further manipulated using the definition of  $K_i$  and  $X_i = \beta y_i + (1 - \beta)x_i$  to obtain the Rachford-Rice equation [22]. Therefore, the non linear system of  $N_s + 1$  equations in the unknowns  $K_i$  and  $\beta$  becomes:

$$\frac{y_i}{x_i} = \frac{\phi_i^L}{\phi_i^V} \frac{p^L}{p^V} \rightarrow \ln K_i - \ln \phi_i^L + \ln \phi_i^V = 0, \quad i = 1, \dots, N_s \quad (3.6)$$

$$\sum_{i=1}^{N_s} \frac{X_i(K_i - 1)}{1 + \beta(K_i - 1)} = 0. \quad (3.7)$$

System of Eqs. (3.6) and (3.7) is solved for given mixture temperature  $T$ , pressure  $p$  and composition  $\mathbf{X}$  (hereafter called  $Tp$  problem). It is very important to keep in mind the temperature, pressure and composition dependency of the unknowns:  $\beta = \beta(T, p, \mathbf{X})$ ,  $\mathbf{y} = \mathbf{y}(T, p, \mathbf{X})$ ,  $\mathbf{x} = \mathbf{x}(T, p, \mathbf{X})$ .

Fugacity coefficients in each phase are determined using Eq. (C.10), where proper phase mole fractions are used as specified above. We underline the fact that in Eq. (3.6), the assumption of  $p^V = p^L = p$  has been used. Accounting for mechanical non equilibrium would mean to provide a model for the pressures ratio, which involves capillarity effects [53,74]. In addition, Eq. (3.6) has been written in logarithmic form in order to improve numerical convergence. Solution of Eqs. (3.6) and (3.7) is also known as VLE problem [22].

Once these basic variables are known, mixture compressibility factor  $Z$  is obtained using its definition in Eq. (2.2) and  $H = E + pV = E + pM/\rho$ , where  $\rho$  and  $E$  are now calculated through Eqs. (3.4) and (3.5). Similarly  $S$ ,  $G$  and  $A$  follow their definitions too. Other phase-related quantities are also available such as the  $\rho^\eta$ ,  $M^\eta$ ,  $Z^\eta$ , where  $\eta = L$  or  $V$ . For example  $\rho^L = \rho^L(T, p, \mathbf{x})$  is obtained by inversion of Eq. (2.1) once  $\mathbf{x}$  is known. Typically for the family of cubic EoS, such as the Peng–Robinson EoS [75], this means to obtain  $Z^L = Z^L(T, p, \mathbf{x})$  first through a cubic, algebraic equation (see Appendix A), and then compute  $\rho^L = pM^L/(Z^L R_u T)$ . If during the solution of the cubic equation in  $Z^L$  multiple real roots arise, that is  $Z^L = [Z_1, Z_2, Z_3]^T$  with  $Z_1 < Z_2 < Z_3$ , the choice is now correctly based on the phase, which is known upfront. For instance if  $Z^L$  is sought, then  $Z^L = Z_1$ . On the contrary, if the vapor phase is being sought, the same procedure applies and  $Z^V = Z_3$ .

Note that the solution  $Z^L = [Z_1, Z_2, Z_3]^T$  would be different if one approaches the problem in the form  $Z = Z(T, p, \mathbf{X})$  because  $\mathbf{x} \neq \mathbf{X}$  in the VLE region. In other words, solving for  $Z = Z(T, p, \mathbf{X})$  assuming “single-fluid” provides a different (erroneous) solution, and in addition, the choice that one would make on the value of  $Z$  in case multiple real roots occur, would be, at the best, based on the minimum Gibbs energy criterion (see Appendix A), if not arbitrary. The minimum Gibbs criterion (which boils down to the Maxwell's criterion for a single component mixture), simply computes the Gibbs energies of the “presumed” phases corresponding to a lower and upper value of the  $Z$  vector, and the phase corresponding to the minimum Gibbs energy is chosen because considered more stable.

However, application of VLE ensures to go beyond that as the imposition of Eq. (3.1) guarantees to reach the true Gibbs energy minimum [61]. That is the same as saying that VLE ensures to reach a *fourth* value of the mixture compressibility factor such that the system is at an even lower value of the Gibbs energy, not reachable with the  $Z = Z(T, p, \mathbf{X})$  (single fluid) approach.

To make an example about this argument, Fig. 2(b) shows the variation of the  $\text{N}_2/\text{C}_6\text{H}_{16}$  mixture compressibility as a function of the nitrogen mole fraction, for  $p = 10$  MPa and  $T = 377.9$  K. This mixture is known to form VLE for a range of values of pressure and temperature [76,77] for which the VLE diagram is represented in Fig. 2(a) along with the chosen  $p = 10$  MPa isobaric line. The two curves agree identically at the extremes, where the single phases occur, whereas substantial variations can be observed in the center values of compressibility where VLE forms. Fig. 2(c) shows the mixture Gibbs energy as a function of the mixture compressibility (essentially  $G$  is plotted along the  $Z$  curves of Fig. 2(b)) for the two approaches. While the two values of  $G$  match in the single phase regions, the value computed with VLE is always smaller than the minimum Gibbs approach in the center region, where VLE occurs, confirming the fact that the mixture tends to spontaneously form a multi-phase system that needs to be taken into account correctly.

Because of the above statements, even when the  $Z = Z(T, p, \mathbf{X})$  problem returns one real value of  $Z$ , it cannot be said that VLE does not form. Instead the whole procedure based on Eq. (3.1) must be followed and only in the case the result of  $\beta = 0$  or  $\beta = 1$  is obtained, one can conclude that only one phase exists, and therefore the single fluid/phase approach theory discussed in Section 2 is perfectly valid [78].

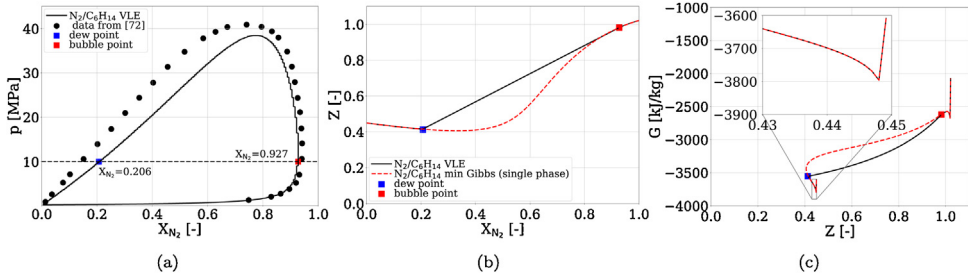


**Fig. 2.** VLE diagram (a), mixture compressibility (b) and Gibbs free energy (c) for a nitrogen/hexane ( $\text{N}_2/\text{C}_6\text{H}_{16}$ ) mixture as a function the amount of  $\text{N}_2$  in mole fractions. The mixture pressure and temperature are maintained fixed in Fig. (b) and (c) at  $p = 10 \text{ MPa}$  and  $T = 377.9 \text{ K}$ , respectively. For these plots, the PR EoS has been used (see also [17]).

Algorithm 1 in Appendix F summarizes the steps to perform in order to compute the phase quantities described above once the VLE problem is solved (description on how to solve the VLE problem is given in [78]). Algorithm 2 instead summarizes the steps to compute some basic mixture quantities. Once again, if VLE does not occur, the well-known single phase RG thermodynamics applies and phases/mixture values become identical.

It is important to emphasize the fact that although these steps are EoS-independent, the specific EoS model employed can have an important effect on the outcome. This can be immediately understood by considering that, for example the Peng-Robinson [75] or the Soave-Redlich-Kwong [84] EoS can exhibit important inaccuracies in the prediction of the fluid density, especially in the liquid phase. For this reason, improved models have been constantly developed in the literature as for example the volume-translated Peng-Robinson EoS [85].

### 3.2. Real gas – VLE thermodynamics: main derivatives

The information provided in the previous section are in general enough for a calculation that requires only minimal output, such as mixture density, compressibility or internal energy. However, in general all the quantities defined in Section 2 are needed. Calculation of higher order thermodynamic variables in the VLE region requires the knowledge of the derivatives of the VLE variables. This can be seen immediately if we consider the calculation of  $c_p$ . Its definition must be the one dictated by thermodynamics. This involves  $H$ , which involves  $E$  and  $\rho$  obtained using Eqs. (3.4) and (3.5). That is:

$$\begin{aligned} c_p &= \left( \frac{\partial H}{\partial T} \right)_{p,\mathbf{x}} = \\ &\quad \text{using Eq. (3.5) for } E \\ &= \left( \frac{\partial \left( E + \frac{pM}{\rho} \right)}{\partial T} \right)_{p,\mathbf{x}} = \beta \left( \frac{\partial E^V}{\partial T} \right)_{p,\mathbf{x}} + (1 - \beta) \left( \frac{\partial E^L}{\partial T} \right)_{p,\mathbf{x}} + \left( \frac{\partial \beta}{\partial T} \right)_{p,\mathbf{x}} (E^V - E^L) - \frac{pM}{\rho^2} \left( \frac{\partial \rho}{\partial T} \right)_{p,\mathbf{x}}. \end{aligned} \quad (3.8)$$

Which is substantially different from a simple blend between phase quantities (refer to Appendix B for more insights). Note that  $E^V = E^V(T, p, \mathbf{y})$ ,  $E^L = E^L(T, p, \mathbf{x})$ , meaning that both  $\mathbf{y} = \mathbf{y}(T, p, \mathbf{X})$  and  $\mathbf{x} = \mathbf{x}(T, p, \mathbf{X})$  dependency on  $T$  need to be taken into account with the derivative. Same applies to the last term for density derivative with respect to temperature. In fact, whenever a temperature/pressure derivative appears, even with fixed mixture “global” composition  $\mathbf{X}$ , phase compositions  $\mathbf{x}$  and  $\mathbf{y}$  vary accordingly, because  $\beta$  varies as well. For this reason, the quantities:

$$\left( \frac{\partial \beta}{\partial T} \right)_{p,\mathbf{x}}, \quad \left( \frac{\partial \beta}{\partial p} \right)_{T,\mathbf{x}}, \quad \left( \frac{\partial \mathbf{x}}{\partial T} \right)_{p,\mathbf{x}}, \quad \left( \frac{\partial \mathbf{y}}{\partial T} \right)_{p,\mathbf{x}}, \quad \left( \frac{\partial \mathbf{x}}{\partial p} \right)_{T,\mathbf{x}}, \quad \left( \frac{\partial \mathbf{y}}{\partial p} \right)_{T,\mathbf{x}}, \quad (3.9)$$

are required to construct all the VLE thermodynamic variables. The last four are vectors of dimension  $N_s$ .

The approach requires to impose Eq. (3.1). First, the following change in variables is made:

$$v_i = \beta y_i, \quad l_i = (1 - \beta)x_i \quad i = 1, \dots, N_s \quad (3.10)$$

such that one can write  $\mathbf{X} = \mathbf{v} + \mathbf{l}$ , with  $\mathbf{v} = \{v_i | i = 1, \dots, N_s\}$  and  $\mathbf{l} = \{l_i | i = 1, \dots, N_s\}$ . In this way, the following identities can be applied since  $\sum_{i=1}^{N_s} y_i = \sum_{i=1}^{N_s} x_i = 1$ :

$$\beta = \sum_{i=1}^{N_s} v_i. \quad (3.11)$$

The variables  $\mathbf{v}$ ,  $T$  and  $p$  are now the independent variables. Determination of all the quantities in Eq. (3.9) essentially requires the knowledge of both temperature and pressure derivatives of the  $v_i$  quantities. The step-by-step derivation on how to do this and details on how to construct all the Eq. (3.9) is provided in Appendix D. Here we focus on the final result, which is given by the solution of two linear systems:

$$\mathbf{A}\chi_T = \mathbf{b}_T, \quad (3.12)$$

$$\mathbf{A}\chi_p = \mathbf{b}_p, \quad (3.13)$$

where:

$$\mathcal{A}_{ik} = \left(1 - \delta_{ki} \frac{x_k}{y_k x_k}\right) + \beta(1 - \beta) \sum_{j=1}^{N_s} \left[ \frac{y_j}{\beta} \left( \frac{\partial \ln \phi_i^V}{\partial y_j} \right)_{T,p,\mathbf{x},\mathbf{y}_j} \left(1 - \frac{\delta_{kj}}{y_j}\right) + \frac{x_j}{1 - \beta} \left( \frac{\partial \ln \phi_i^L}{\partial x_j} \right)_{T,p,\mathbf{x},\mathbf{x}_j} \left(1 - \frac{\delta_{jk}}{x_j}\right) \right], \quad (3.14)$$

$$b_{T,i} = \beta(1 - \beta) \left[ \left( \frac{\partial \ln \phi_i^V}{\partial T} \right)_{p,\mathbf{x},\mathbf{y}} - \left( \frac{\partial \ln \phi_i^L}{\partial T} \right)_{p,\mathbf{x},\mathbf{x}} \right], \quad (3.15)$$

$$b_{p,i} = \beta(1 - \beta) \left[ \left( \frac{\partial \ln \phi_i^V}{\partial p} \right)_{T,\mathbf{x},\mathbf{y}} - \left( \frac{\partial \ln \phi_i^L}{\partial p} \right)_{T,\mathbf{x},\mathbf{x}} \right], \quad (3.16)$$

$$\chi_{T,k} = \left( \frac{\partial v_k}{\partial T} \right)_{p,\mathbf{x}}, \quad (3.17)$$

$$\chi_{p,k} = \left( \frac{\partial v_k}{\partial p} \right)_{T,\mathbf{x}}, \quad (3.18)$$

with  $i, k = 1, \dots, N_s$  and  $\delta_{ij}$  the Kronecker delta.

Note that  $\mathcal{A}$  is the same for both systems and thus it can be assembled/inverted only once. All the fugacity coefficients (frozen) derivatives appearing in Eqs. (3.14)–(3.16) can be easily computed using an EoS model, thus the above formulation can be applied to any EoS that is capable to provide the fugacity coefficient and its derivatives. It is interesting to underline the fact that the  $v_k$  derivatives lead to a linear system. This is due to the effect that all species-related properties are not independent but they are linked to each other. Additional important formulas are the phase molar masses derivatives with respect to pressure and temperature:  $\left(\frac{\partial M^V}{\partial T}\right)_{p,\mathbf{x}}$ ,  $\left(\frac{\partial M^V}{\partial p}\right)_{T,\mathbf{x}}$ ,  $\left(\frac{\partial M^L}{\partial T}\right)_{p,\mathbf{x}}$  and  $\left(\frac{\partial M^L}{\partial p}\right)_{T,\mathbf{x}}$ . These are also provided in [Appendix D](#). Algorithm 3 in [Appendix F](#) summarizes the steps that are required to compute all the quantities of Eq. (3.9). Note, this requires that VLE exists and it is known in terms of  $\beta, \mathbf{x}, \mathbf{y}$ .

### 3.3. Real gas – VLE thermodynamics: mixture and phase derivatives

With the above formulas, many additional properties for the mixture, as well as the phases separately, can be constructed. Here we discuss only some relevant quantities, for brevity. Additional details are given in [Appendix D](#). The mixture density and internal energy derivatives with respect to temperature and pressure are given below:

$$\begin{aligned} & \text{Using Eq. (3.4)} \\ & \left( \frac{\partial \rho}{\partial T} \right)_{p,\mathbf{x}} = -\frac{\rho^2}{M} \left\{ \left( \frac{\partial \beta}{\partial T} \right)_{p,\mathbf{x}} \left( \frac{M^V}{\rho^V} - \frac{M^L}{\rho^L} \right) + \frac{\beta}{\rho^{V2}} \left[ \rho^V \left( \frac{\partial M^V}{\partial T} \right)_{p,\mathbf{x}} - M^V \left( \frac{\partial \rho^V}{\partial T} \right)_{p,\mathbf{x}} \right] + \right. \\ & \quad \left. + \frac{1 - \beta}{\rho^{L2}} \left[ \rho^L \left( \frac{\partial M^L}{\partial T} \right)_{p,\mathbf{x}} - M^L \left( \frac{\partial \rho^L}{\partial T} \right)_{p,\mathbf{x}} \right] \right\}, \end{aligned} \quad (3.19)$$

$$\begin{aligned} & \left( \frac{\partial \rho}{\partial p} \right)_{T,\mathbf{x}} = -\frac{\rho^2}{M} \left\{ \left( \frac{\partial \beta}{\partial p} \right)_{T,\mathbf{x}} \left( \frac{M^V}{\rho^V} - \frac{M^L}{\rho^L} \right) + \frac{\beta}{\rho^{V2}} \left[ \rho^V \left( \frac{\partial M^V}{\partial p} \right)_{T,\mathbf{x}} - M^V \left( \frac{\partial \rho^V}{\partial p} \right)_{T,\mathbf{x}} \right] + \right. \\ & \quad \left. + \frac{1 - \beta}{\rho^{L2}} \left[ \rho^L \left( \frac{\partial M^L}{\partial p} \right)_{T,\mathbf{x}} - M^L \left( \frac{\partial \rho^L}{\partial p} \right)_{T,\mathbf{x}} \right] \right\}. \end{aligned} \quad (3.20)$$

$$\left( \frac{\partial E}{\partial T} \right)_{p,\mathbf{x}} = \left( \frac{\partial \beta}{\partial T} \right)_{p,\mathbf{x}} (E^V - E^L) + \beta \left( \frac{\partial E^V}{\partial T} \right)_{p,\mathbf{x}} + (1 - \beta) \left( \frac{\partial E^L}{\partial T} \right)_{p,\mathbf{x}}, \quad (3.21)$$

$$\left( \frac{\partial E}{\partial p} \right)_{T,\mathbf{x}} = \left( \frac{\partial \beta}{\partial p} \right)_{T,\mathbf{x}} (E^V - E^L) + \beta \left( \frac{\partial E^V}{\partial p} \right)_{T,\mathbf{x}} + (1 - \beta) \left( \frac{\partial E^L}{\partial p} \right)_{T,\mathbf{x}}. \quad (3.22)$$

All of above require the knowledge of the VLE derivatives of Eq. (3.9), as well as specific, phase-related derivatives, such as  $(\partial \rho^L / \partial p)_{T,\mathbf{x}}$  or  $(\partial E^L / \partial T)_{p,\mathbf{x}}$  and similar. The latter are derived in [Appendix D](#). Note that these derivatives do not correspond to the ones directly derived from the EoS and the departure functions because the variation of VLE quantities is also involved and must be taken into account using the total differential concept (see [Appendix D](#)). For example  $(\partial \rho^L / \partial p)_{T,\mathbf{x}}$  is not equal to  $(\partial \rho^L / \partial p)_{T,\mathbf{x},\mathbf{x}}$ , which is the one (easily) computed from the EoS and their difference is related to the existence of all the Eq. (3.9) in the VLE region (see Eq. (D.25) for this specific example). Algorithm 5 provides the necessary steps to compute the derivatives in each phase, while Algorithm 4 provides the final steps to compute additional derivatives for the VLE mixture, up to specific heats, isothermal compressibility, isobaric expansivity and speed of sound. The last quantities to compute are the partial molar volume and enthalpy in the VLE region. These are discussed in the next section.

### 3.4. Real gas – VLE thermodynamics: partial molar quantities

We begin from the definition of partial molar volume of Eq. (2.7). Using Eq. (3.2) for the definition of the total volume one gets:

$$V_i = \left( \frac{\partial \bar{V}}{\partial N_i} \right)_{T,p,\mathbf{N}_i} = \left( \frac{\partial \bar{V}^V}{\partial N_i} \right)_{T,p,\mathbf{N}_i} + \left( \frac{\partial \bar{V}^L}{\partial N_i} \right)_{T,p,\mathbf{N}_i} \quad i = 1, \dots, N_s. \quad (3.23)$$

Since  $\bar{V}^\eta = \bar{V}^\eta(T, p, \sigma)$ , where:

$$\sigma = \{\sigma_i \mid i = 1, \dots, N_s\} = \begin{cases} \mathbf{N}^L = \{N_i^L \mid i = 1, \dots, N_s\} & \text{if } \eta = L \\ \mathbf{N}^V = \{N_i^V \mid i = 1, \dots, N_s\} & \text{if } \eta = V \end{cases}, \quad (3.24)$$

$$\sigma = \begin{cases} N^L = \sum_{i=1}^{N_s} N_i^L & \text{if } \eta = L \\ N^V = \sum_{i=1}^{N_s} N_i^V & \text{if } \eta = V \end{cases}, \quad (3.25)$$

and  $N_i^L, N_i^V$  are the number of moles of species  $i$  in each phase. The total differential of the extensive volume in the generic phase  $\eta$  writes:

$$d\bar{V}^\eta = \left( \frac{\partial \bar{V}^\eta}{\partial T} \right)_{p,\sigma} dT + \left( \frac{\partial \bar{V}^\eta}{\partial p} \right)_{T,\sigma} dp + \sum_{k=1}^{N_s} \left( \frac{\partial \bar{V}^\eta}{\partial \sigma_k} \right)_{T,p,\sigma_k} d\sigma_k, \quad (3.26)$$

where  $\sigma_k = \{\sigma_i \mid i = 1, \dots, N_s, i \neq k\}$  has been defined to make it consistent with the previous notation. Because the partial molar quantities are by definition taken at constant temperature and pressure, the first two terms in Eq. (3.26) vanish. Next, by evaluating the variation of Eq. (3.26) with respect to the generic  $N_i$ , one gets immediately for both phases:

$$\left( \frac{\partial \bar{V}^\eta}{\partial N_i} \right)_{T,p,\mathbf{N}_i} = \sum_{k=1}^{N_s} \left( \frac{\partial \bar{V}^\eta}{\partial \sigma_k} \right)_{T,p,\sigma_k} \left( \frac{\partial \sigma_k}{\partial N_i} \right)_{T,p,\sigma_k, \mathbf{N}_i} \quad i = 1, \dots, N_s, \quad (3.27)$$

In both phases, the summation term contains the product between two quantities:  $(\partial \bar{V}^\eta / \partial \sigma_k)_{T,p,\sigma_k}$  which describes how the phase extensive volume changes with an infinitesimal addition of moles of species  $k$  in the phase  $\eta$ , and the term  $(\partial \sigma_k / \partial N_i)_{T,p,\sigma_k, \mathbf{N}_i}$ , which describes how much the number of moles of species  $k$  in the phase  $\eta$  changes for an infinitesimal addition of number of “total” moles of species  $i$  in the mixture. This is the most challenging term to compute and it is going to be the subject of the next discussion. Given the number of crucial steps involved, we report the step-by-step derivation in [Appendix E](#) and we limit ourselves here to show only the final result. The vapor contribution  $(\partial N_k^V / \partial N_i)_{T,p,\mathbf{N}_k^V, \mathbf{N}_i}$  of Eq. (3.27) is obtained by solving  $N_s$  times the following linear system in the unknown vector  $\chi_N^{(i)}$ :

$$\mathbf{C} \chi_N^{(i)} = \mathbf{b}_N^{(i)} \quad i = 1, \dots, N_s, \quad (3.28)$$

where:

$$c_{kj} = \sum_{s=1}^{N_s} \left[ \left( \frac{\partial \ln \phi_k^L}{\partial x_s} \right)_{T,p,\mathbf{x}_s} \left( \frac{\delta_{sj} - x_s}{1 - \beta} \right) + \left( \frac{\partial \ln \phi_k^V}{\partial y_s} \right)_{T,p,\mathbf{y}_s} \left( \frac{\delta_{sj} - y_s}{\beta} \right) \right] + \frac{1}{x_k} \frac{\delta_{kj} - x_k}{1 - \beta} + \frac{1}{y_k} \frac{\delta_{kj} - y_k}{\beta}, \quad (3.29)$$

$$b_{N,k}^{(i)} = \sum_{j=1}^{N_s} \delta_{ji} \left\{ \sum_{s=1}^{N_s} \left[ \left( \frac{\partial \ln \phi_k^L}{\partial x_s} \right)_{T,p,\mathbf{x}_s} \left( \frac{\delta_{sj} - x_s}{1 - \beta} \right) \right] + \frac{\delta_{ji}}{x_k} \left( \frac{\delta_{kj} - x_k}{1 - \beta} \right) \right\}, \quad (3.30)$$

$$\chi_{N,j}^{(i)} = \left( \frac{\partial N_j^V}{\partial N_i} \right)_{T,p,\mathbf{N}_j^V, \mathbf{N}_i}. \quad (3.31)$$

However, given the fact that the matrix  $\mathbf{C}$  does not depend on  $i$ , the matrix inversion itself must be done only once for all the unknowns. On the other hand, the liquid contribution  $(\partial N_k^L / \partial N_i)_{T,p,\mathbf{N}_k^V, \mathbf{N}_i}$  of Eq. (3.27) is easily obtained from the vapor contribution by exploiting mass continuity (see [Appendix E](#)). Algorithm 6 summarizes the steps to compute the partial molar volume for each species in the mixture, in case VLE occurs. If VLE does not occur, the single phase formula applies.

Next, we derive the formula to compute the partial molar enthalpy in the VLE region. Starting from the definition of Eq. (2.7) and use the definition of enthalpy, one gets:

$$h_i = pV_i + \left( \frac{\partial \bar{E}^V}{\partial N_i} \right)_{T,p,\mathbf{N}_i} + \left( \frac{\partial \bar{E}^L}{\partial N_i} \right)_{T,p,\mathbf{N}_i} \quad i = 1, \dots, N_s. \quad (3.32)$$

Eq. (3.32) requires the knowledge of the partial molar volume and the vapor and liquid extensive internal energies variations with respect to the  $i$ -th component mole number. To compute these, application of their total differential is again needed. The details are reported in [Appendix E](#).

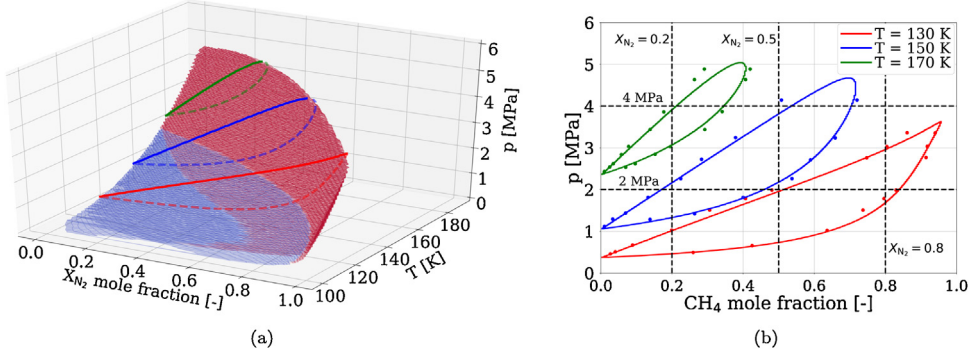


**Fig. 3.** (a) 3D VLE diagram for the  $N_2/CH_4$  mixture. The three iso-thermal VLE domes are the same represented also in (b) where dots represent data taken from [79]. Dashed and dotted lines indicate the iso-composition and the iso-baric conditions along with data is analyzed further. (For interpretation of the references to color in this figure legend, the reader is referred to the web version of this article.)

Finally, an approximate method to compute partial molar quantities is proposed. Given that one can compute the respective phase-related molar volume and enthalpy  $V_i^\eta$  and  $h_i^\eta$  using Eq. (2.7), and given the fact that:

$$V^V = \sum_{i=1}^{N_s} V_i^V y_i, \quad V^L = \sum_{i=1}^{N_s} V_i^L x_i, \quad h^V = \sum_{i=1}^{N_s} h_i^V y_i, \quad h^L = \sum_{i=1}^{N_s} h_i^L x_i, \quad (3.33)$$

must be satisfied, the mixture approximate two-phase partial molar quantities are computed as:

$$V_i = \frac{\beta y_i V_i^V + (1 - \beta) x_i V_i^L}{X_i}, \quad i = 1, \dots, N_s \quad (3.34)$$

$$h_i = \frac{\beta y_i h_i^V + (1 - \beta) x_i h_i^L}{X_i}, \quad i = 1, \dots, N_s. \quad (3.35)$$

Which can be easily proven to satisfy the required condition that  $V = \sum_{i=1}^{N_s} V_i X_i$  and  $H = \sum_{i=1}^{N_s} h_i X_i$ .

#### 4. Results

In this section, the analytical derivatives described in Section 3 are tested and validated. Before doing so, several notes must be given:

- an EoS has to be declared. In this work we are going to use the Peng-Robinson [75] (PR) EoS along with the mixing rule of Harstad et al. [49]. This means that whenever a specific EoS derivative is needed, such as for the calculation of the departure functions in Eqs. (C.1)–(C.4) or the fugacity coefficient in Eq. (C.10) and its derivatives required, for example, in Eqs. (3.14)–(3.16), the PR model is used. These derivatives can be easily found in other resources [22,49,53,63,75] and therefore are not repeated here, for brevity;
- comparison of thermodynamic properties is conducted by employing three different methods: (a) multi-phase analytical derivatives of Section 3, (b) single-phase analytical derivatives of Section 2 and (c) an hybrid, approximate method that we refer here as “frozen VLE”. This method is made of two steps: one “exact” step which consists of the calculation of VLE identically to method (a) and a second step which uses the same analytical derivatives of Section 3 in the VLE region, but it assumes that all the VLE derivatives, such as  $(\partial\beta/\partial p)_{p,\mathbf{x}}$ ,  $(\partial\beta/\partial T)_{T,\mathbf{x}}$ ,  $(\partial M^V/\partial T)_{p,\mathbf{x}}$ ,  $(\partial\zeta_i/\partial p)_{T,\mathbf{x},\zeta_i}$  are zero. This will reflect into the fact that “total” derivatives match with frozen derivatives as for example  $(\partial E^\eta/\partial T)_{p,\mathbf{x}} \equiv (\partial E^\eta/\partial T)_{p,\mathbf{x},\zeta}$  related to Eq. (D.32). This applies to all the mixture, as well as phase properties discussed in Section 3.

This approach leads to the calculation of some thermodynamic properties in the VLE by merely blending phase specific properties as  $\Sigma = \beta\Sigma^V + (1 - \beta)\Sigma^L$ , where  $\Sigma$ ,  $\Sigma^V$  and  $\Sigma^L$  represent the generic property in the mixture, vapor phase and liquid phase, respectively. A proof of this statement is given in Appendix B;

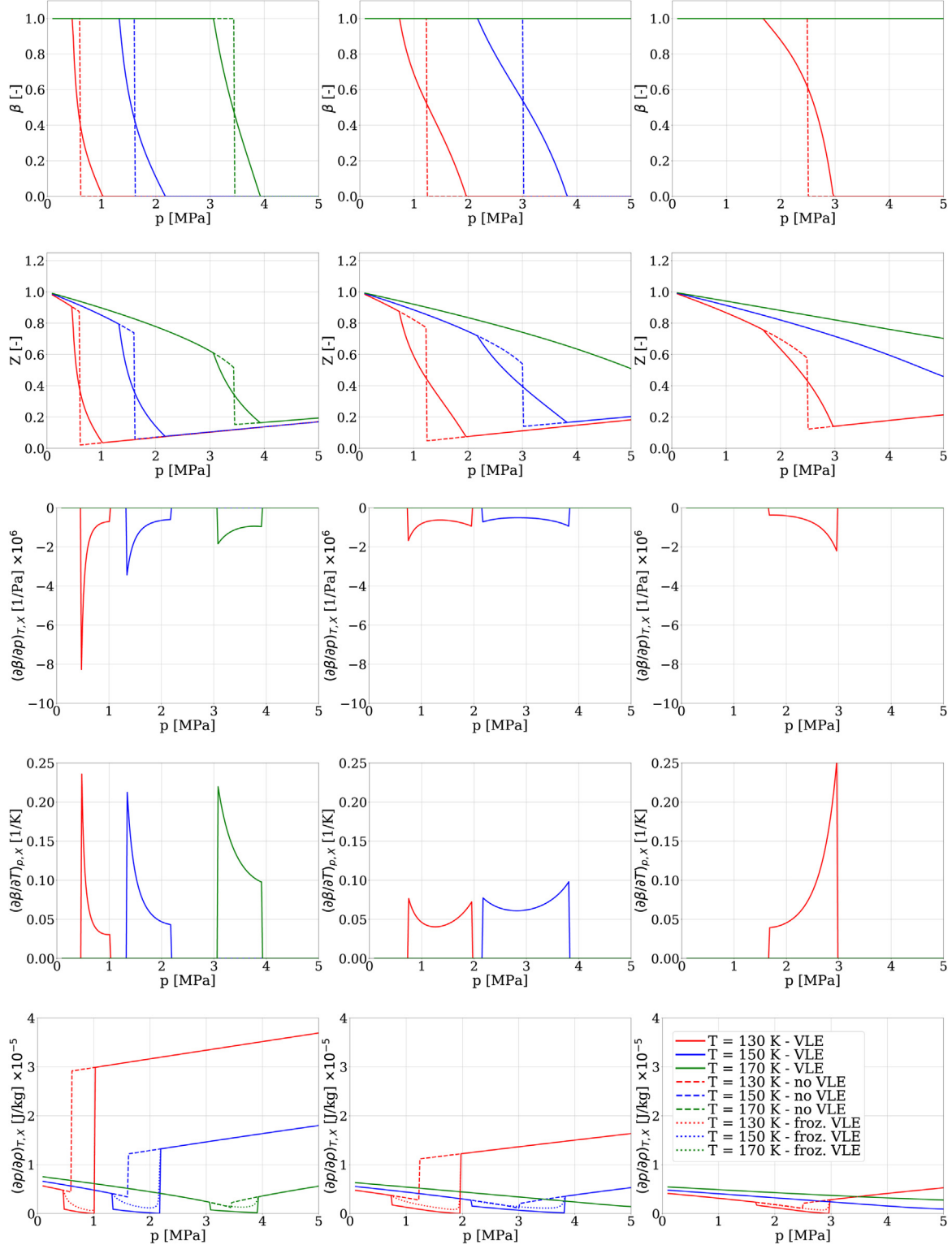
- evaluation of partial molar quantities is performed with exact (Eq. (3.23) and Eq. (3.32)) and approximate (Eqs. (3.34) and (3.35)) formulas. Note that approximation of Eqs. (3.34) and (3.35) does not necessarily imply the frozen VLE assumption as these are independent simplifications. Nevertheless we still include this under the “frozen” VLE method in order to avoid unnecessary multiplication of terminology;

We specify that the solution of the VLE problem at given temperature, pressure and composition required in 2 can be borrowed from any related publication in the literature. For this specific work, we use the one described by Michelsen [78] which involves an hybrid method between the Successive Substitution Iteration (SSI) and the full Newton methods respectively. The Tangent-Plane Distance (TPD) analysis is also used to test the mixture phase stability. This approach has been already used in [17]. For additional information, the reader is referred to [54,78].

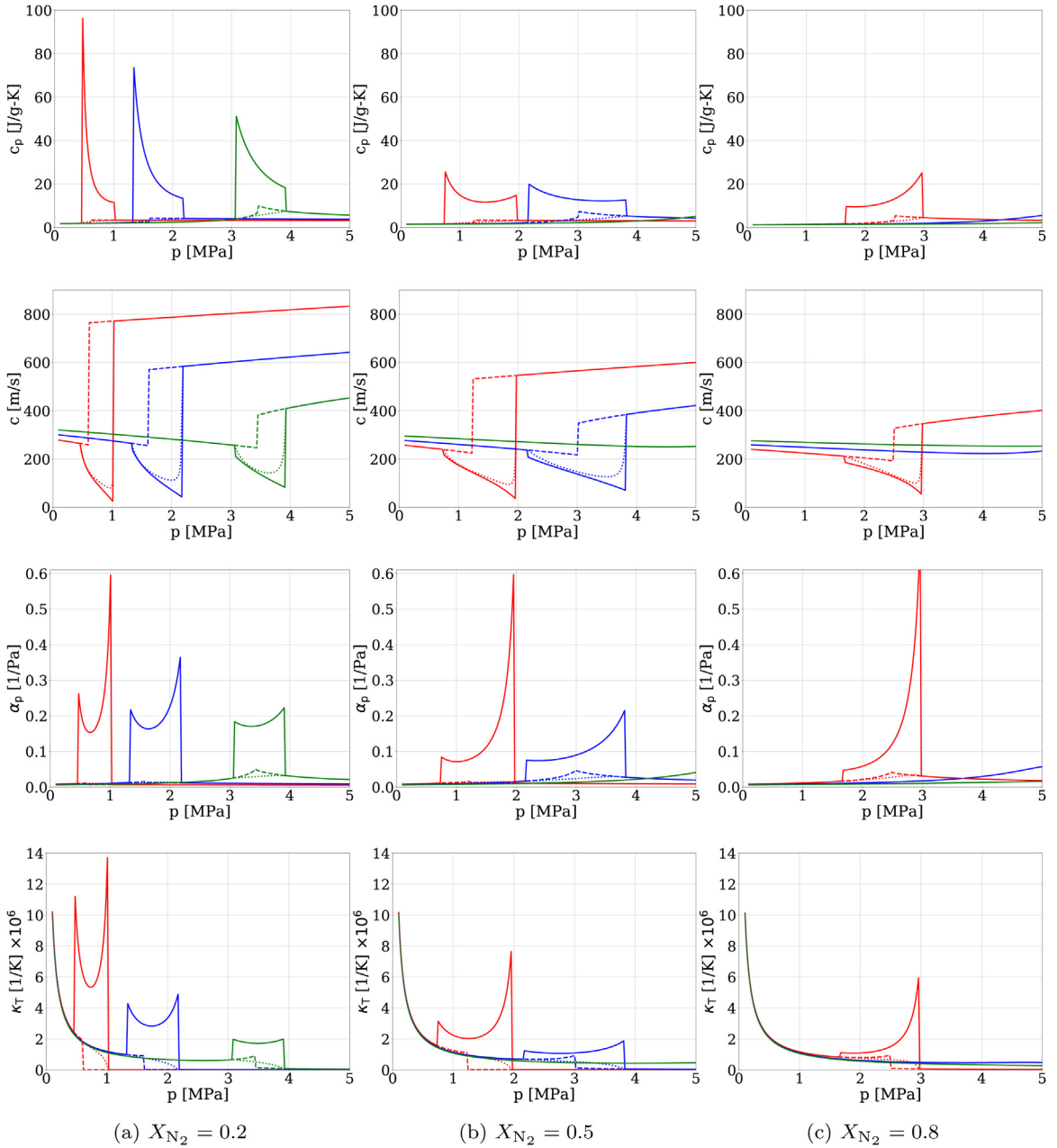
In order to proceed with the calculation of thermodynamic derivatives, reference solutions of VLE are required. In this work we are going to consider two binary mixtures, one ternary and one very complex mixture of 14 species. The starting point will be always the VLE diagram validated against data published elsewhere. Next, iso-baric, iso-thermal and iso-composition lines are examined in terms of thermodynamic properties calculated with the different models.

#### 4.1. Binary mixture # 1: N<sub>2</sub>/CH<sub>4</sub>

The first binary mixture considered is N<sub>2</sub>/CH<sub>4</sub>. First, the 3D VLE diagram is provided in Fig. 3(a) along with iso-thermal slices, separately displayed in Fig. 3(b). The red and blue shaded areas in Fig. 3(a) represent the VLE dome boundaries where the mixture pseudo-phase is considered vapor-like or liquid-like, respectively. The pseudo transition here is considered to happen at the condition where  $Z^* = 2.5B_{mp}/R_u T$ ,



**Fig. 4.** Iso-composition results for the N<sub>2</sub>/CH<sub>4</sub> mixture. Variables are organized column-wise with respect to the fixed amount of N<sub>2</sub> mole fraction. Variables labeled as  $(\cdot) \times 10^x$  indicate that the represented data is multiplied by the factor  $10^x$ . The legend is shown only once and is valid for all the plot series.

**Fig. 4.** (Continued)

where  $B_m$  is the mixture-based, volume-shift coefficient appearing at the denominator of the repulsive term in the (PR) EoS (for the notation, the reader is referred to [17]). If  $Z \geq Z^*$ , the mixture is considered in its pseudo-vapor phase, otherwise it is considered in its pseudo-liquid phase. This represents just a reference definition outside the VLE dome and does not affect any of the results or conclusions discussed in the following. The thermodynamic models are evaluated along iso-composition and iso-baric lines sketched in Fig. 3(b).

Fig. 4 shows the iso-composition properties of the mixture taken at different amount of N<sub>2</sub> according to Fig. 3(b). Each variable here is able to show different features and therefore the importance of the full analytical VLE model. For example the  $\beta$  field shows that the variations with respect to the pressure (and indirectly temperature) can be much different as the composition is varied. Particularly, despite the monotonic decreasing trend observed in all cases, the first derivative with respect to the pressure can change drastically, up to the point where the second derivative changes sign for the  $X_{N_2} = 0.5$  case. This is immediately visible in the  $(\partial\beta/\partial p)_{T,X}$  and  $(\partial\beta/\partial T)_{p,X}$  pictures. This has a huge consequence on all the thermodynamic variables that use these derivatives, depending on whether the VLE or the frozen VLE model is used. While the disagreement between the VLE and the frozen VLE model in  $(\partial p/\partial\rho)_{T,X}$  and  $c$  is somewhat less pronounced with a higher error occurring near the phase boundaries, the error for  $c_p$ ,  $\alpha_p$  and  $\kappa_T$  is huge, with trends that are also drastically different. For example in  $c_p$ , the frozen VLE model cannot take into account for sudden jumps near phase boundaries because of the fact that  $(\partial\beta/\partial T)_{p,X}$  is assumed to be zero, however when multiplied by  $(E^V - E^L)$  according to Eq. (3.8) it introduces a big effect, which is not taken into account in the frozen VLE case. This is also true because the approximation  $(\partial\rho/\partial T)_{p,X} \approx (\partial\rho/\partial T)_{p,X}\zeta$  and similarly for other involved derivatives is made in the frozen case.

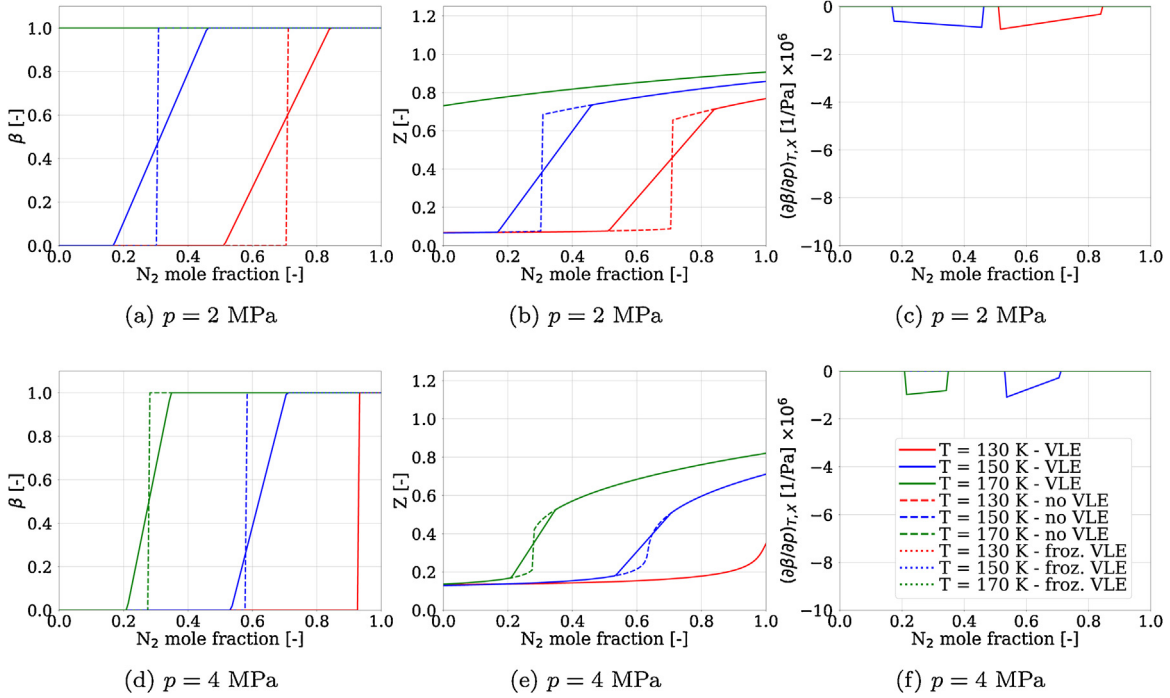


**Fig. 5.** Iso-baric results for the  $\text{N}_2/\text{CH}_4$  mixture. Variables:  $\beta$ ,  $Z$  and  $d\beta/dp$ .

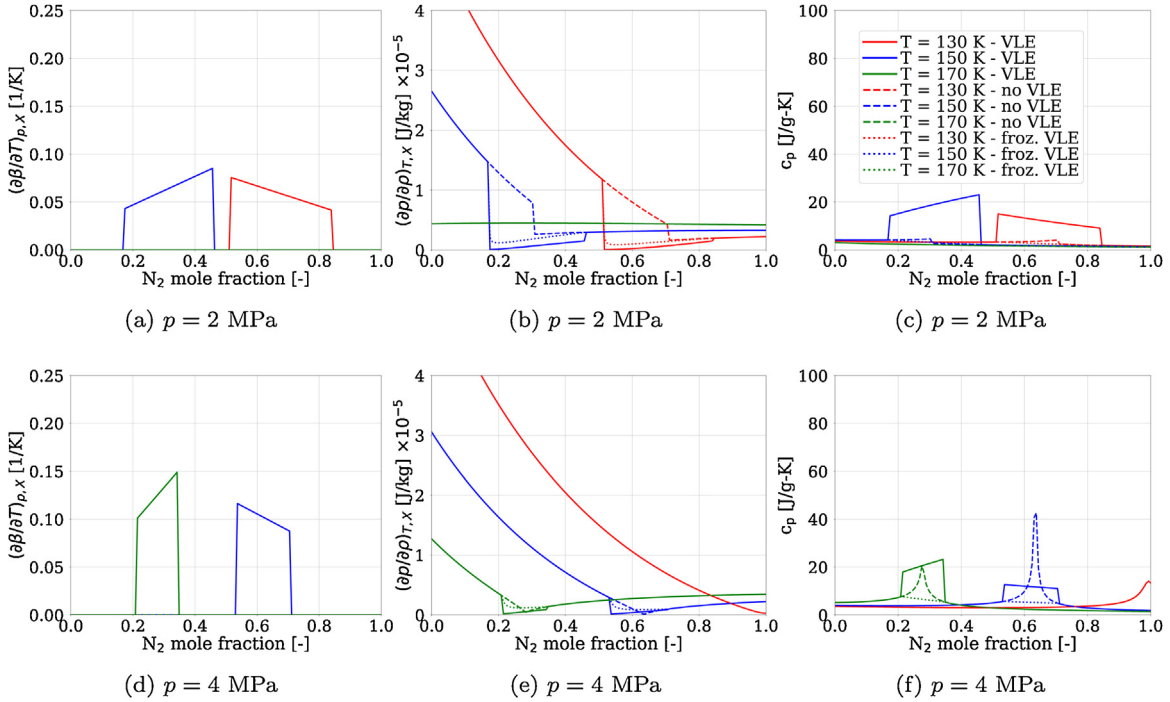


**Fig. 6.** Iso-baric results for the  $\text{N}_2/\text{CH}_4$  mixture. Variables:  $d\beta/dT$ ,  $dp/d\rho$  and  $c_p$ .

In all cases, the no VLE model performs poorly in the 2-phase region, with the tendency to produce unphysical discontinuities in the variables and their derivatives. This is due to the fact that the minimum Gibbs criterion suddenly jumps between the phases and selects a completely different compressibility root, as visible in the  $Z$  pictures. This choice creates a discontinuity that reflects in all variables and that does not exist in the VLE case where the fields of  $\beta$  and  $Z$  are continuous, with discontinuous first derivatives at the phase boundary. Finally, in the single-phase regions all the models agree as expected because all the mathematical assumptions match with the real physics being computed.

Figs. 5–7 show relevant mixture variables obtained along the iso-baric lines according to Fig. 3(b) where analogous observations can be made. Fig. 8 and 9 illustrate the partial molar volume and partial molar enthalpy obtained for the iso-composition (only  $X_{\text{N}_2} = 0.5$  shown) and iso-baric (only  $p = 4 \text{ MPa}$  shown) case, respectively. The pictures are differentiated according to the thermodynamic model indicated in the label. Each picture shows the partial molar property for each species (such as  $V_{\text{N}_2}$ ), the overall mixture property (such as  $V = M/\rho$ )

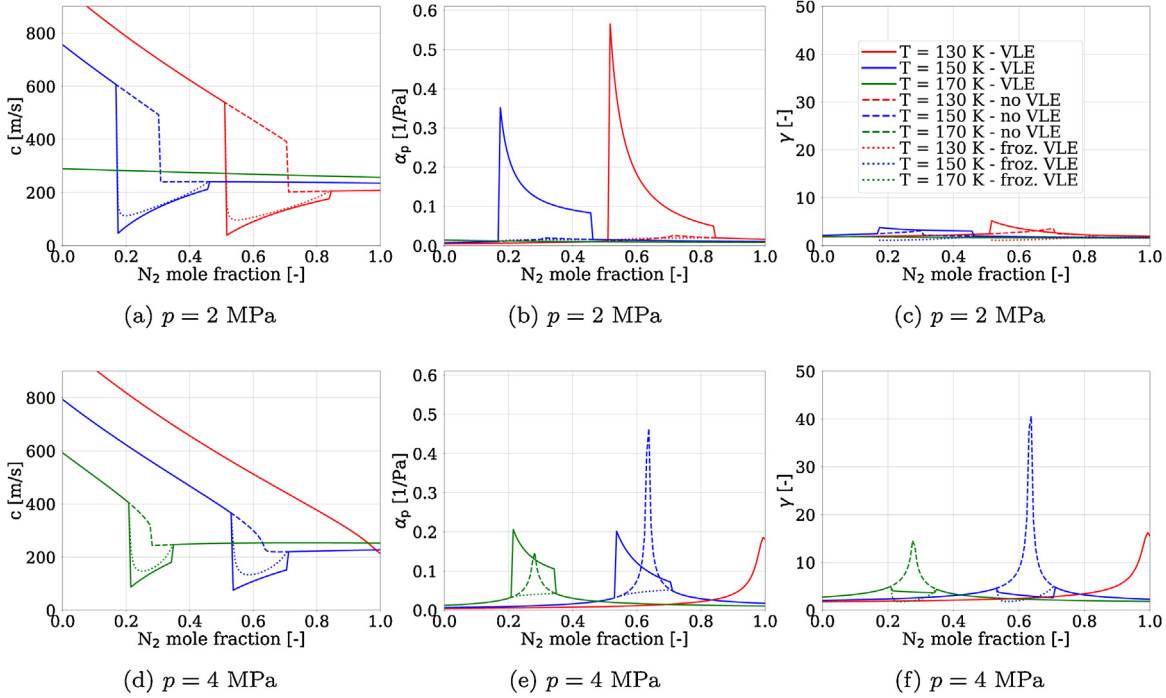


**Fig. 7.** Iso-baric results for the  $\text{N}_2/\text{CH}_4$  mixture. Variables:  $c$ ,  $\alpha_p$  and  $\gamma$ . (Labels are same as Fig. 5)

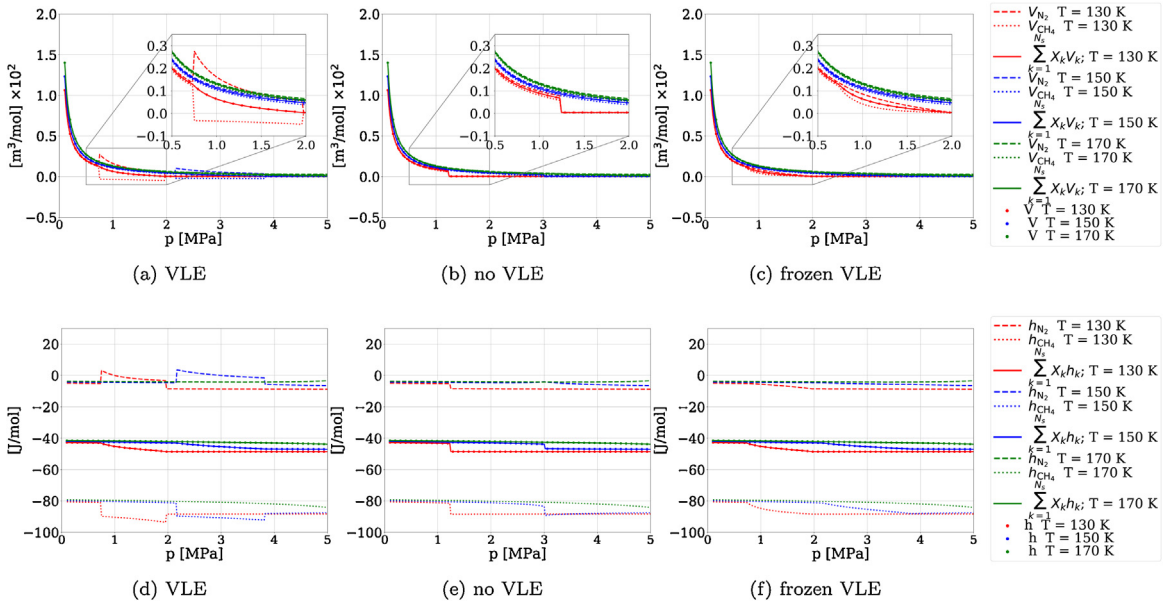


**Fig. 8.** Partial molar volume (top row) and enthalpy (bottom row) computed along iso-composition line  $X_{\text{N}_2} = 0.5$  using the three different thermodynamic models.

and the thermodynamic constraint that has to be satisfied by definition (such as  $\sum_{k=1}^{N_s} X_k V_k = V$ ) at each examined temperature according to Fig. 3(b). The goal of this is to conclude the following information: while the thermodynamic constraint is satisfied in all conditions, the individual partial molar properties can exhibit significant departures depending on the thermodynamic model. This leads to the conclusion that although the model provided by Eqs. (3.34) and (3.35) can give a reasonable estimation of the actual property, errors can be made with the computation of mass and energy diffusion terms. As a result, this can play an important role in problems where such terms are dominant as for example in heat transfer studies.

#### 4.2. Binary mixture # 2: $\text{CH}_4/\text{CO}_2$

The second mixture under consideration is another binary mixture with  $\text{CH}_4/\text{CO}_2$ . For this mixture, interaction parameters of  $k_{ij} = 0.048$ ,  $i \neq j$  are used. Fig. 10(a) shows the iso-thermal VLE diagram with reference data. In order to avoid repetition with the previous results, for this case we show the analyses conducted at iso-baric conditions, for which the respective VLE diagram is illustrated in Fig. 10(b). Furthermore in Figs. 11 and 12 we limit ourselves to show the relevant mixture properties for the iso-composition taken at  $X_{\text{CH}_4} = 0.1$  (left

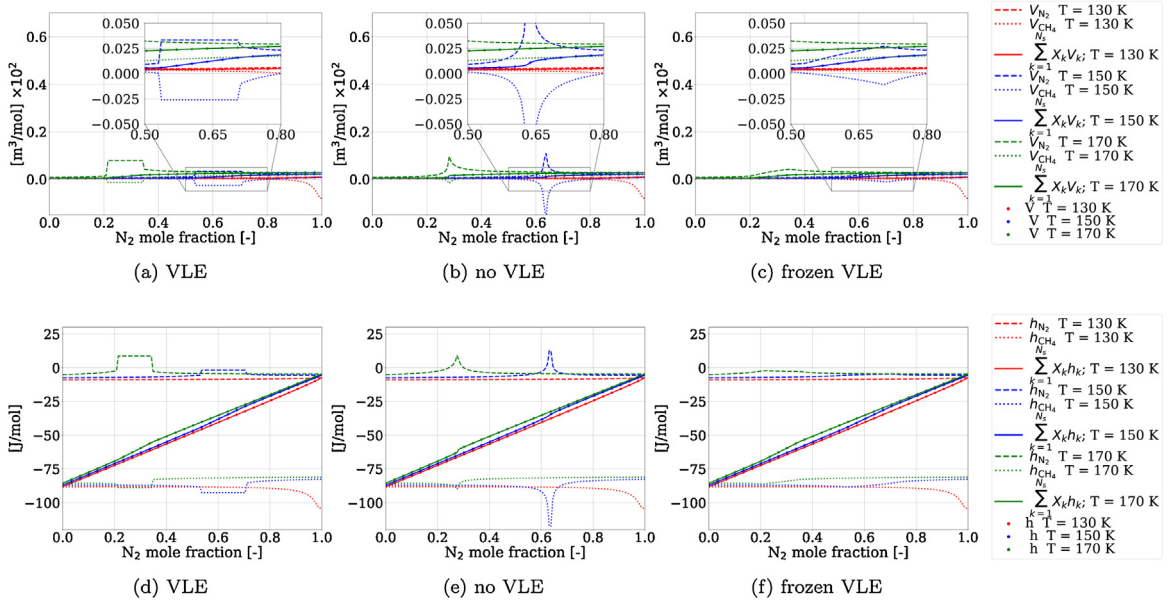


**Fig. 9.** Partial molar volume (top row) and enthalpy (bottom row) computed along the iso-baric line  $p = 4$  MPa using the three different thermodynamic models.

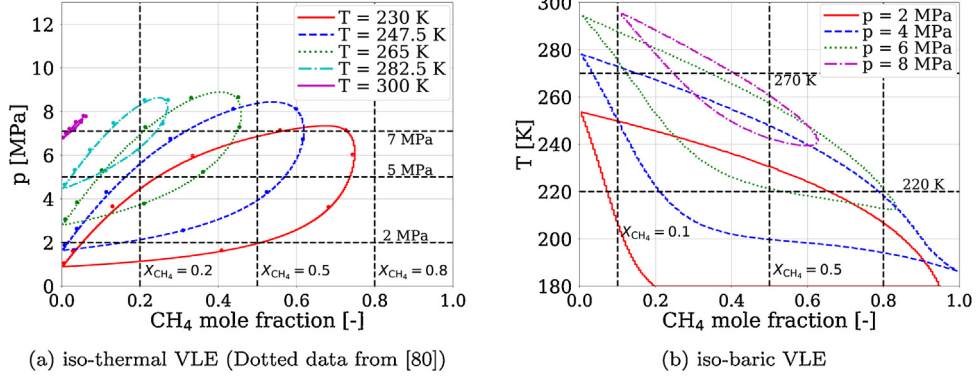


**Fig. 10.** (a) Iso-thermal and (b) iso-baric VLE diagrams for CH<sub>4</sub>/CO<sub>2</sub> mixture [80].

column) and iso-thermal taken at  $T = 220$  K (right column) conditions only, for brevity (analyses conducted onto other lines leads to the exact conclusions). Similarly to what discussed earlier, the first derivatives of the main VLE properties play a crucial role for the mixture thermodynamic derivatives. The departures among the thermodynamic models observed for  $c_p$  and  $\gamma$  are simply unacceptable and even the error in the speed of sound between the VLE and the frozen VLE model appears larger than the previous case and it increases as pressure increases. Other observations regarding the no VLE model and the behavior in the single-phase regions remain the same, leading to the same conclusions as before. The same discussion holds for the partial molar quantities as well, here displayed in Fig. 13 for the iso-composition case of  $X_{CH_4} = 0.1$  only, for brevity.

#### 4.3. Ternary mixture: CH<sub>4</sub>/N<sub>2</sub>/C<sub>2</sub>H<sub>6</sub>

The third case discussed is that of a ternary mixture involving species CH<sub>4</sub>/N<sub>2</sub>/C<sub>2</sub>H<sub>6</sub>. The ternary VLE diagram for various iso-baric and iso-thermal conditions is shown in Fig. 14 along with reference data, for validation. Data is analyzed for all cases along different “test lines” which consider only mixture composition variations. These lines are shown in Fig. 14 for reference and are obtained as follows:

- test line 1:  $X_{N_2} = 0.2, X_{CH_4} \in [0.0, 1.0 - X_{N_2}], X_{C_2H_6} = 1.0 - X_{N_2} - X_{CH_4};$
- test line 2:  $X_{N_2} \in [0.0, 1.0 - X_{CH_4}], X_{CH_4} = 0.2, X_{C_2H_6} = 1.0 - X_{N_2} - X_{CH_4};$
- test line 3:  $X_{N_2} = 1.0 - X_{CH_4} - X_{C_2H_6}, X_{CH_4} \in [0.0, 1.0 - X_{C_2H_6}], X_{C_2H_6} = 0.2.$

For the sake of paper length, we limit ourselves to show in Figs. 15 and 16 only the results pertaining to the test line 3 relative to the conditions of Fig. 14(d) and Fig. 14(f). Other cases led to the same conclusions and therefore are omitted here. Again we observe the same

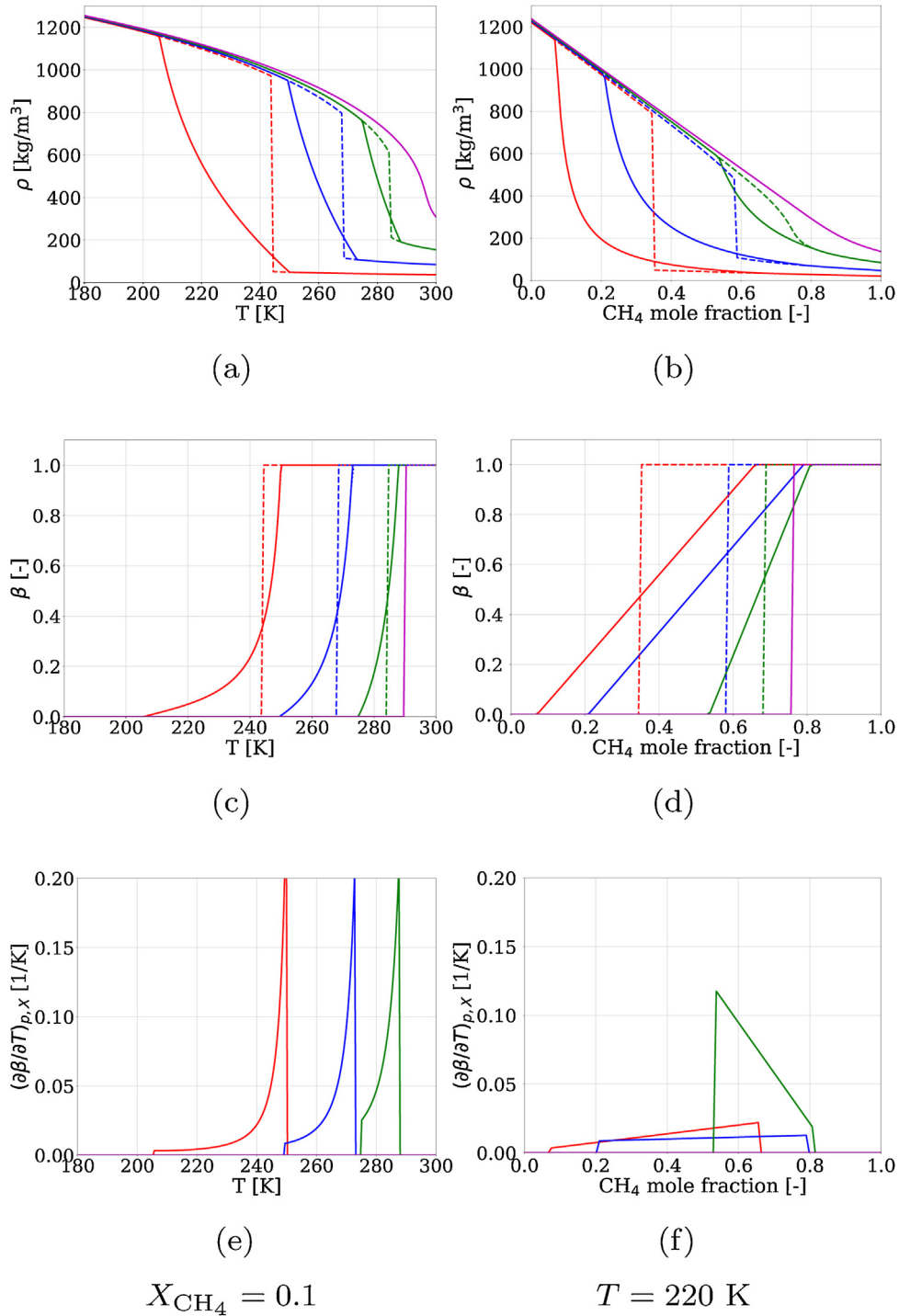


**Fig. 11.** Iso-composition (left column) and iso-thermal (right column) results set # 1 ( $\rho$ ,  $\beta$  and  $\partial\beta/\partial T$ ) for the  $\text{CH}_4/\text{CO}_2$  mixture.

features in thermodynamic variables as done before, leading to the conclusion that frozen VLE thermodynamics is an assumption that produces big approximations in the two-phase regions.

#### 4.4. Prudhoe bay mixture

The final mixture considered for this study is the Prudhoe bay gas [82], which consists of 14 species involving different hydrocarbons, including  $\text{CH}_4$ , as well as  $\text{O}_2$ ,  $\text{N}_2$  and  $\text{CO}_2$ . The VLE diagram of this mixture is provided in [82] for a constant composition (also provided in [82]) and by varying temperature and pressure. This VLE data is first used to further validate the present multi-phase equilibrium model in Fig. 17(a). Next, iso-baric lines indicated in the same picture are analyzed and compared with available data in the literature. Fig. 17(b)

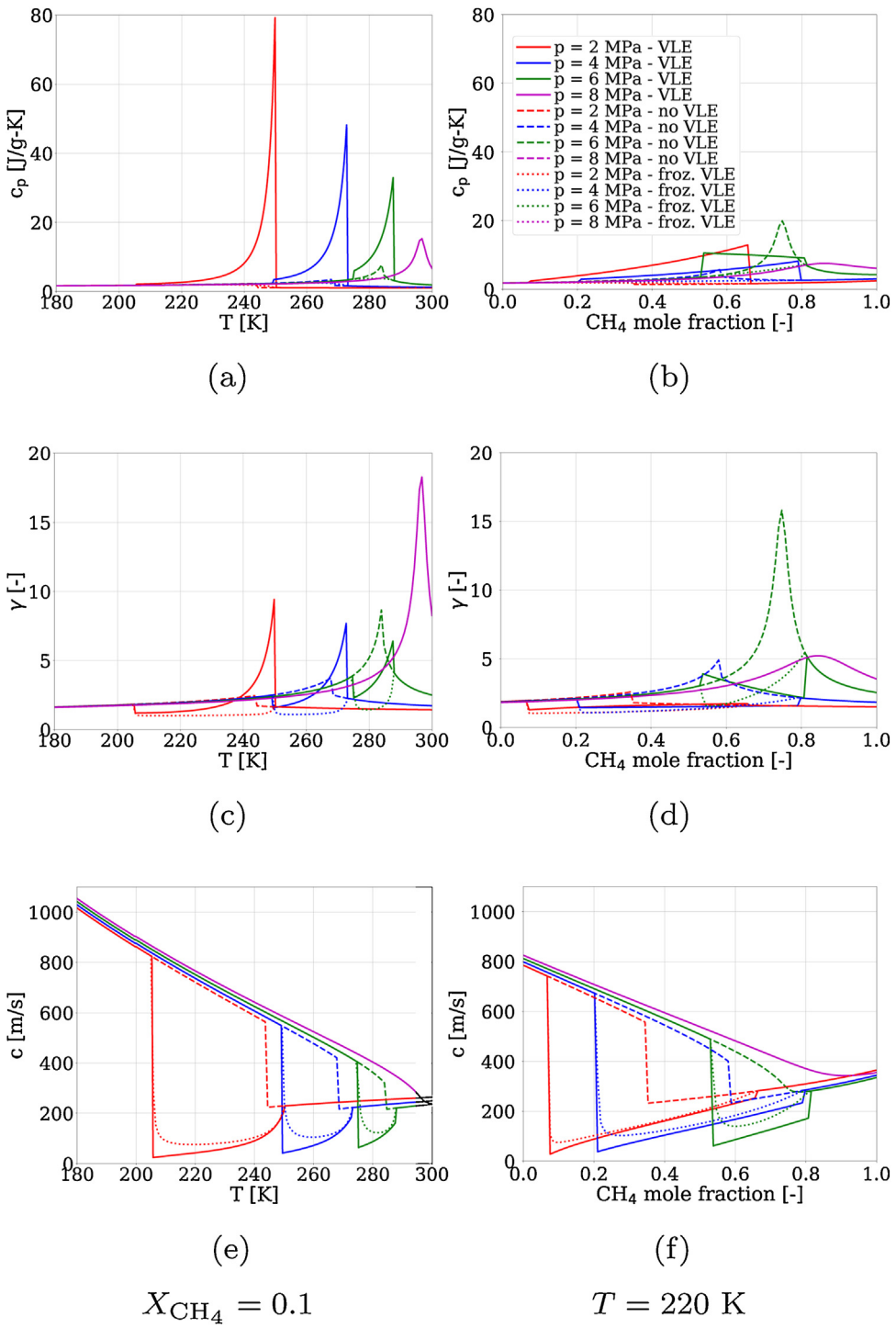


**Fig. 12.** Iso-composition (left column) and iso-thermal (right column) results set # 2 ( $c_p$ ,  $\gamma$  and  $c$ ) for the  $\text{CH}_4/\text{CO}_2$  mixture.

shows the comparison of the calculated speed of sound at fixed pressure of 1 MPa using all three thermodynamic models (indicated in the picture legend). While the single-phase (no VLE) model again shows very low performances for the same reasons discussed earlier, we again observe the frozen VLE model to show acceptable results, with reasonably good capability to capture the mixture phase boundaries. Still, an error of about 300% is achieved for the lowest peak, which can be unacceptable, depending on the application. Next, Fig. 17(d) displays more iso-baric curves for the speed of sound, now including reference data, the frozen VLE model and the Wood's equation [83]. The purpose of this picture is to essentially compare the frozen VLE assumption and the Wood's equation. It is apparent that the difference between the two approaches is significant and leads to the following conclusions: (a) the frozen VLE model performs much better than the simple Wood's correlation; given that both require the knowledge of the VLE data (*i.e.*  $\beta$ ,  $x_i$  and  $y_i$ ), the computational cost of both models is about the same because no VLE derivatives are required, however significant improvement can be achieved, (b) the reason why

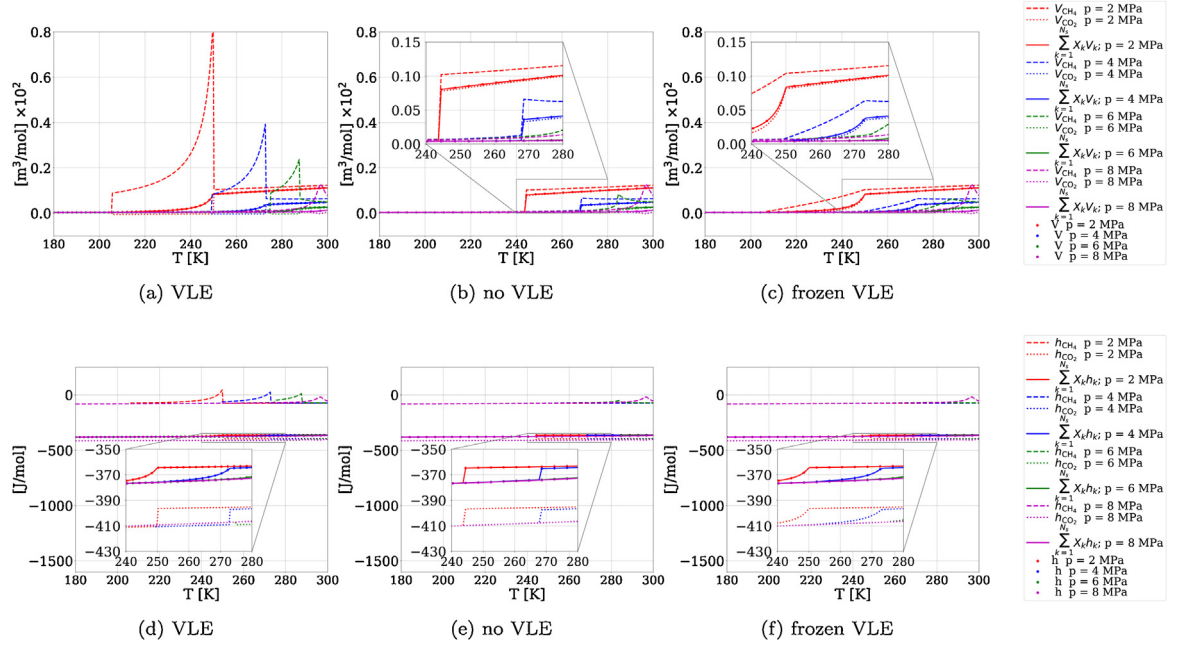


**Fig. 13.** Partial molar volume (top row) and enthalpy (bottom row) computed along iso-composition line  $X_{CH_4} = 0.1$  using the three different thermodynamic models.

the frozen VLE model performs better compared to the Wood's equation is related to some non-linear terms between the phase properties that are neglected in the Wood's correlation. These appear to be crucial to capture the phase boundaries reasonably well, although the full VLE model contains all the necessary information to get the correct result. More insights between the frozen VLE assumption and the Wood's equation are given in Appendix B. In the same appendix we also provide some additional explanation regarding the reason why the frozen VLE assumption performs better on the speed of sound and not as good in the specific heats calculation (see Fig. 17(f)). Fig. 17(e) shows the comparison of the isentropic compressibility  $\kappa_s$  with reference data computed with the different models. Analogous discussion made for the speed of sound holds. Finally, Fig. 17(c) and (d) show the mixture enthalpy and specific heat at constant pressure for the same iso-baric lines. It is immediate to observe the following:

- the single-phase (no VLE) model shows the same features discussed earlier. This model is incorrect to predict properties within the multi-phase region, as expected;
- the frozen VLE model predicts the same value of enthalpy as the full VLE model (lines are overlapped). This is not surprising since the multi-phase enthalpy is only a function of the VLE variables and not their derivatives;
- on the other hand, the value of  $c_p$  shows huge departures between the VLE and the frozen VLE model, again due to the lack of representation of correct phase-boundaries trends introduced by the VLE derivatives which are not taken into account by the frozen VLE method. Once again this underlines the fact that with the frozen VLE model, big errors and inconsistencies can be introduced and, depending on the type of analysis being performed, this can play a crucial role in the outcome;
- in the real single-phase zone represented by the 8 MPa curves, all the models collapse to a unique (correct) solution.

#### 4.5. Considerations on numerical versus analytical derivatives for the calculation of VLE properties

The present thermodynamic model for two-phase equilibrium systems represents the analytical version of a numerical approach initially proposed by [20] and later used by [68] and [17]. One can compute all the thermodynamic properties in a VLE system by construct finite differences in the thermodynamic space of all the derivatives discussed in this work. Although consistency and correctness is achieved [17,20,68], particular attention has to be given near the phase boundaries, where the perturbation of the current VLE state to construct the numerical derivative can fall outside the actual VLE dome, affecting the overall result of the derivative itself in an erroneous manner. This issue is just briefly pointed out in [20] and only in [17] a specific phase sensor is proposed in order to avoid it. Nevertheless, the sensor itself can be problem-dependent and case-specific tuning procedure might be required upfront. On the other hand, the present analytical model completely eliminates the issue because once the VLE is found, ( $\beta \in (0, 1)$ ), the derivatives are computed in an analytical manner, without any perturbation of the current state. Another advantage of the present model is related to the gain in the calculation speed to compute all the properties. Although the present model requires substantial amount of floating point operations, including linear system solutions with associated matrix inversions (see Appendix F), it is still computationally more efficient than solving for the numerical derivatives as in [17,20,68] because the latter requires to solve additional VLE problems of Eqs. (3.6) and (3.7) in the perturbed temperature or pressure states to construct the derivatives with finite differences. To illustrate this point, Table 1 reports the computational cost, in terms of time to compute all the thermodynamic properties after the solution of the VLE problem with both the numerical [17,20,68] and the analytical (present) models. Here we can observe that at least a speed up of 30% is achieved with the present model, even in the Prudhoe gas case which contains 14 species, confirming the advantage of the present model over the numerical model. Note that both models have the same computational time when no VLE calculations are involved.

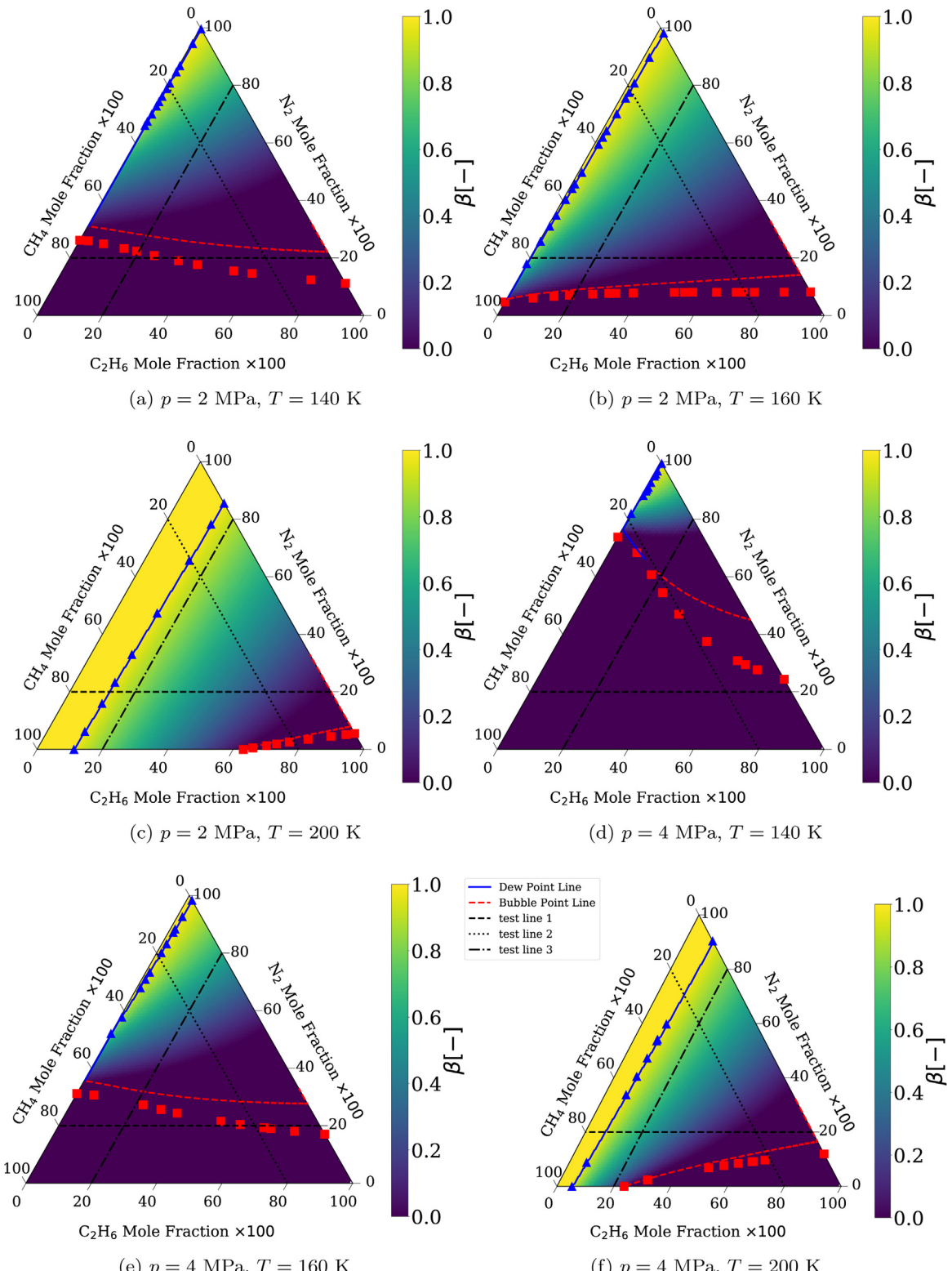


**Fig. 14.** Ternary VLE diagrams for  $\text{CH}_4/\text{N}_2/\text{C}_2\text{H}_6$  mixture at different pressures and temperatures. Solid blue and dashed red lines indicate the dew and bubble point contours. Symbols are taken from [81]. Black lines indicate the compositional variations chosen for numerical experiments (see legend). (For interpretation of the references to color in this figure legend, the reader is referred to the web version of this article.)

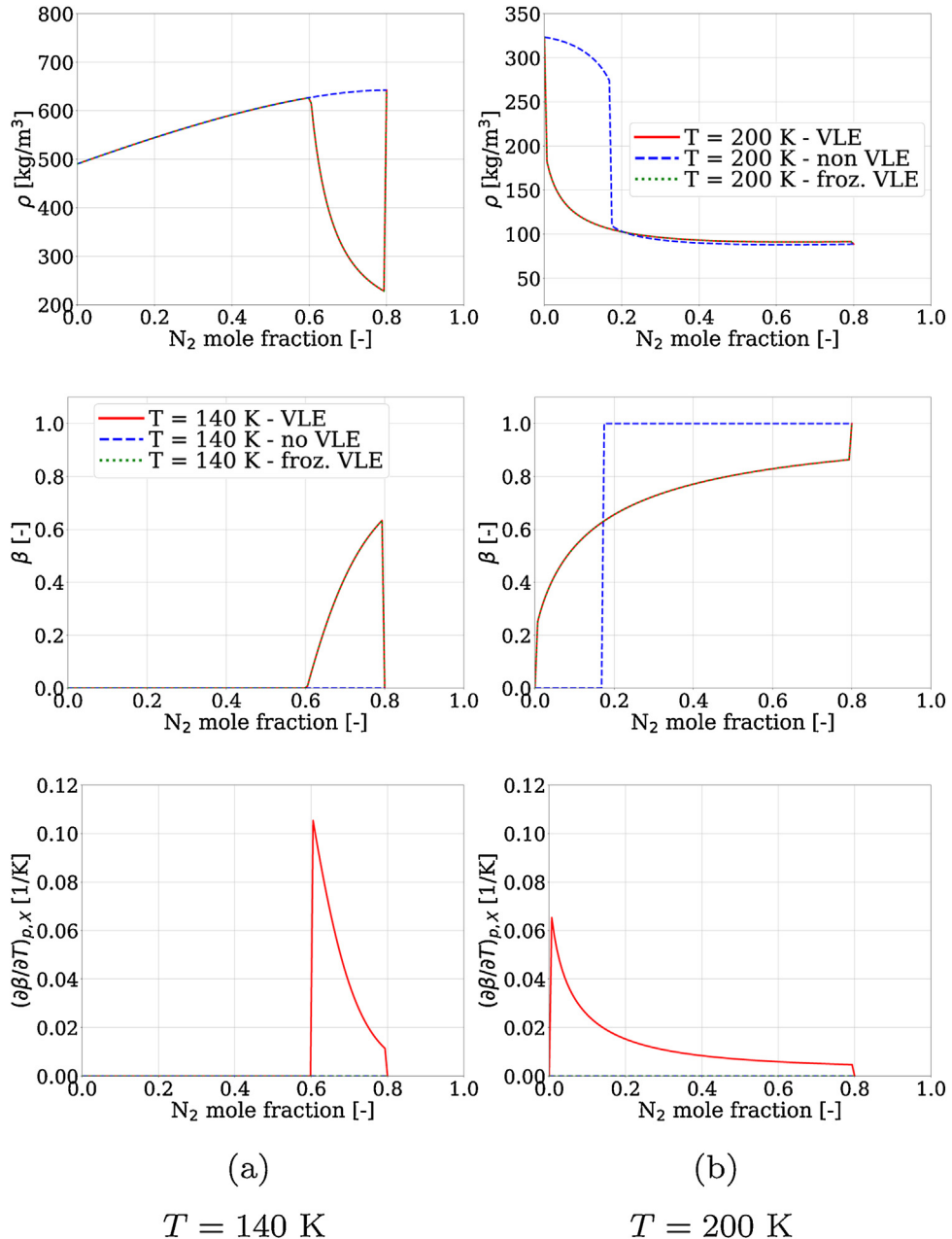


**Fig. 15.** Ternary mixture relevant properties set # 1 ( $\rho$ ,  $\beta$  and  $\partial\beta/\partial T$ ) analyzed along the test line # 3 of Fig. 14 for  $p=4\text{ MPa}$  and varying the temperature:  $T=140\text{ K}$  (left column) and  $T=200\text{ K}$  (right column). These correspond to the test line # 3 of Fig. 14(d) and (f) respectively.

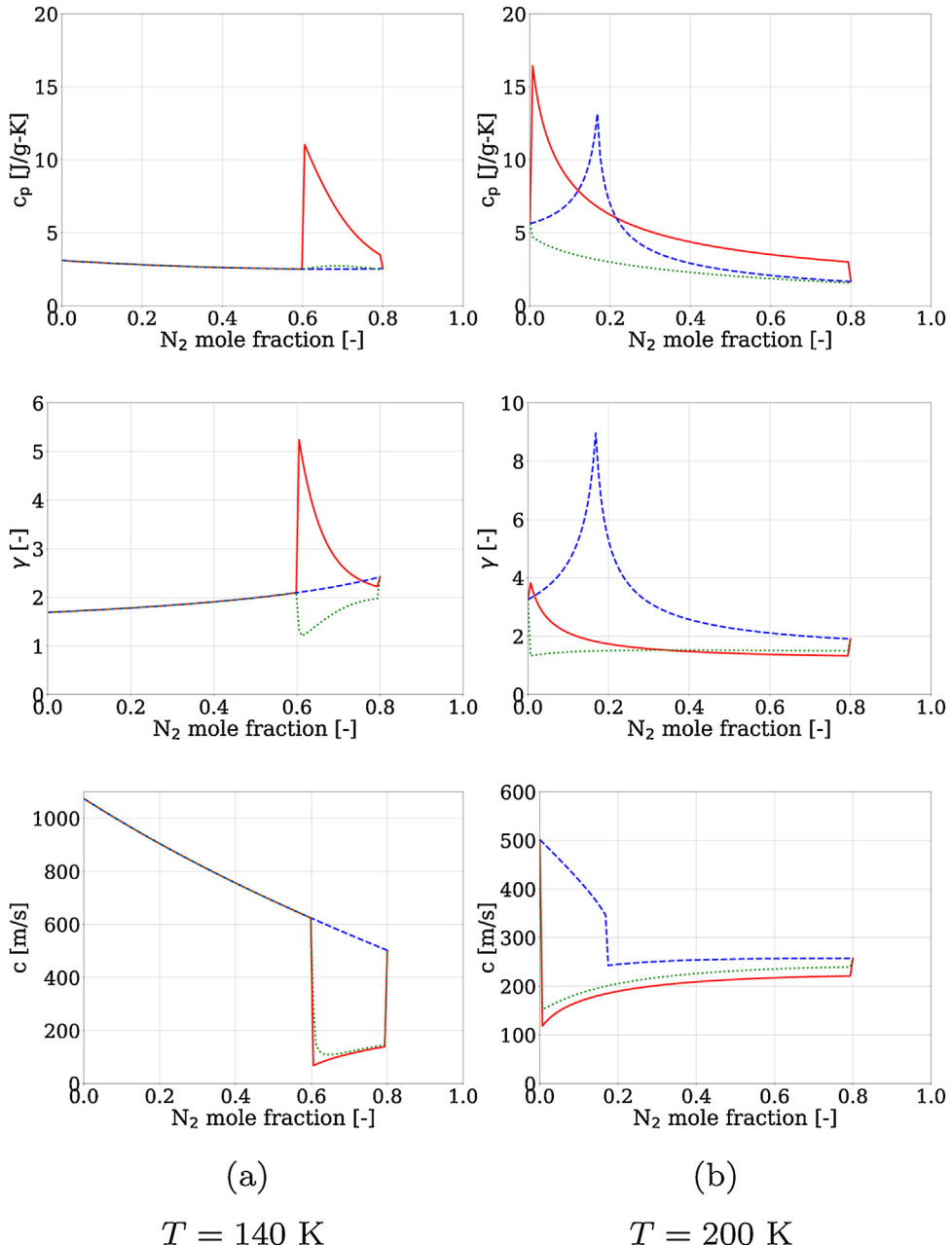


**Fig. 16.** Ternary mixture relevant properties set # 2 ( $c_p$ ,  $\gamma$  and  $c$ ) analyzed along the test line # 3 of Fig. 14 for  $p=4\text{ MPa}$  and varying the temperature:  $T=140\text{ K}$  (left column) and  $T=200\text{ K}$  (right column). These correspond to the test line # 3 of Fig. 14(d) and Fig. 14(f) respectively.

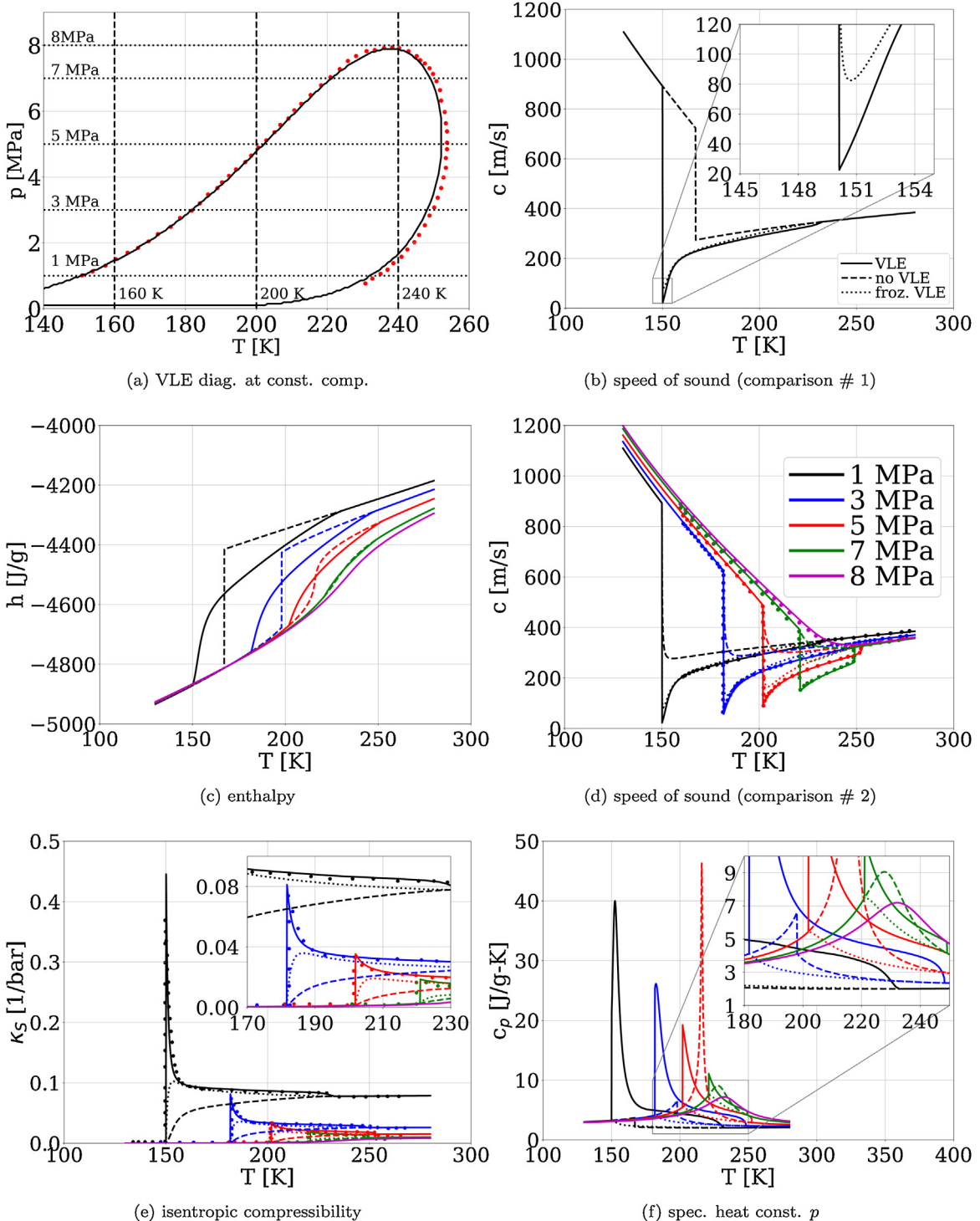


**Fig. 17.** (a) VLE diagram of the Prudhoe gas at fixed composition (dotted data taken from [82]), (b) speed of sound comparison along  $p=1$  MPa with different models: (—) VLE, (---) no VLE, (...) frozen VLE (cfr. Fig. 17(a)), (c) Iso-baric enthalpy (cfr. Fig. 17(a)), (d) speed of sound along iso-baric lines (Fig. 17(a), dotted data taken from [82]), (e) isentropic compressibility along iso-baric lines (Fig. 17(a), dotted data taken from [20]), (f) specific heat and constant pressure (cfr. Fig. 17(a)). In (b) and (d) solutions are as follows: (—) VLE, (...) frozen VLE, (---) Wood's equation [83]. In c) and f) solutions are as follows: (—) VLE, (...) frozen VLE, no VLE (---).

**Table 1**

Comparison of computational times to calculate all the thermodynamic properties between the numerical model [20] and the analytical model (present work). Data is collected based on the mixtures considered above.

Mixture	Case	Details	Num. points computed	Numer. model [ms]	Analyt. model [ms]	Time reduction (%)
N <sub>2</sub> /CH <sub>4</sub>	iso-X 0.2	T=130 K, p ∈ [0.1, 6] MPa	2000	43.19	27.54	-36.23
N <sub>2</sub> /CH <sub>4</sub>	iso-X 0.2	T=150 K, p ∈ [0.1, 6] MPa	2000	55.23	30.19	-45.33
N <sub>2</sub> /CH <sub>4</sub>	iso-X 0.2	T=170 K, p ∈ [0.1, 6] MPa	2000	58.53	30.79	-47.39
N <sub>2</sub> /CH <sub>4</sub>	iso-X 0.5	T=130 K, p ∈ [0.1, 6] MPa	2000	72.88	33.83	-53.58
N <sub>2</sub> /CH <sub>4</sub>	iso-X 0.5	T=150 K, p ∈ [0.1, 6] MPa	2000	91.71	36.68	-60.00
N <sub>2</sub> /CH <sub>4</sub>	iso-X 0.5	T=170 K, p ∈ [0.1, 6] MPa	2000	23.46	23.46	-0.00
N <sub>2</sub> /CH <sub>4</sub>	iso-p 2 MPa	T = 130 K, X <sub>N<sub>2</sub></sub> ∈ [0, 1]	2000	92.14	35.13	-61.87
N <sub>2</sub> /CH <sub>4</sub>	iso-p 2 MPa	T = 150 K, X <sub>N<sub>2</sub></sub> ∈ [0, 1]	2000	75.41	32.22	-57.27
N <sub>2</sub> /CH <sub>4</sub>	iso-p 2 MPa	T = 170 K, X <sub>N<sub>2</sub></sub> ∈ [0, 1]	2000	23.24	23.24	-0.00
N <sub>2</sub> /CH <sub>4</sub>	iso-p 4 MPa	T = 130 K, X <sub>N<sub>2</sub></sub> ∈ [0, 1]	2000	27.39	27.39	-0.00
N <sub>2</sub> /CH <sub>4</sub>	iso-p 4 MPa	T = 150 K, X <sub>N<sub>2</sub></sub> ∈ [0, 1]	2000	70.25	36.69	-47.77
N <sub>2</sub> /CH <sub>4</sub>	iso-p 4 MPa	T = 170 K, X <sub>N<sub>2</sub></sub> ∈ [0, 1]	2000	52.66	28.93	-45.06
Ternary	test line # 3	T=140 K, p=4MPa	2000	180.61	76.94	-57.39
Ternary	test line # 3	T=200 K, p=4MPa	2000	253.13	60.62	-76.05
Prudhoe gas	iso-T 160 K	p ∈ [0.1, 8] MPa	2000	460.36	335.54	-27.11
Prudhoe gas	iso-T 200 K	p ∈ [0.1, 8] MPa	2000	1209.98	675.03	-44.21
Prudhoe gas	iso-T 240 K	p ∈ [0.1, 8] MPa	2000	1545.95	730.33	-52.76
Prudhoe gas	iso-T 260 K	p ∈ [0.1, 8] MPa	2000	253.18	253.18	-0.00
Prudhoe gas	iso-p 1 MPa	T ∈ [140, 260] K	2000	993.88	580.04	-41.63
Prudhoe gas	iso-p 3 MPa	T ∈ [140, 260] K	2000	1013.89	563.43	-44.42
Prudhoe gas	iso-p 5 MPa	T ∈ [140, 260] K	2000	1017.69	548.64	-46.08
Prudhoe gas	iso-p 7 MPa	T ∈ [140, 260] K	2000	1231.07	596.13	-51.57
Prudhoe gas	iso-p 8 MPa	T ∈ [140, 260] K	2000	511.55	511.55	-0.00

## 5. Conclusions

In this work we provided a complete analytical thermodynamic model to describe multi-phase mixtures under phase equilibrium assumption. This framework is of particular interest when simulating fluid-dynamics, as well as heat transfer problems involving multi-component mixtures at conditions far from ideal, where a non-ideal equation of state is required to predict the presence of at least two separate phases. The present analytical framework represents an exact thermodynamic model when only two phases are considered and when no capillarity effects are taken into account. However both assumptions can be relaxed and the model can easily incorporate such additional features. Validation and analysis of this model is made by using available data in the literature of mixtures with increasing complexity. The analytical model is compared against two additional methods namely the frozen VLE method that assumes all the VLE derivatives to be zero, and the no VLE or single-fluid method which does not allow to have multi-phase conditions at a given state but only single-phase conditions. The results clearly indicate that no matter the mixture complexity, the simplified models do not have the capability to correctly evaluate the thermodynamic properties in the two-phase region. Particularly while the no VLE model already predicts the basic thermodynamic properties erroneously (and obviously their derivatives), the frozen VLE model agrees exactly with the full VLE method for basic thermodynamic properties (such as density, enthalpy and so on), but performs poorly on all other variables that should take into account VLE derivatives, such as  $(\partial\beta/\partial T)_{p,X}$ ,  $(\partial\beta/\partial p)_{T,X}$  and similar. As a result, the strong departures between the models can have an unpredictable impact over the whole simulation outcome and should be avoided. Additionally, we show that the present model has superior performances than a corresponding fully numerical approach concerning the computational expense where a speedup of 30% or more is achieved irrespective of the mixture complexity.

## Funding

This study was funded by US Air Force Office of Scientific Research under a research grant FA9550-15-1-0033 (Dr. Mitat Birkan, Program Manager). The author also acknowledges Prof. Jerry Seitzman for the helpful discussions about the topic.

## Conflict of interest

The authors declare that they have no conflict of interest.

## Appendix A. Minimum Gibbs criterion for compressibility root selection

For a cubic EoS, substitution of Eq. (2.2) into Eq. (2.1) leads to a unique cubic equation in the compressibility factor in the form  $a_1Z^3 + a_2Z^2 + a_3Z + a_4 = 0$ , which can be solved in an analytical manner. First the two quantities are computed:

$$Q = \frac{A^2 - 3B}{9}, \quad R = \frac{2A^3 - 9AB + 27C}{54}. \quad (\text{A.1})$$

Where  $A = a_2/a_1$ ,  $B = a_3/a_1$  and  $C = a_4/a_1$ . Then a decision is made out of the sign of the quantity  $Q^3 - R^2$ :

- if  $Q^3 - R^2 < 0$ , the cubic equation has only one real root:

$$Z = -\text{sign}(R) \left\{ \left[ (R^2 - Q^3)^{1/2} + |R| \right]^{1/3} + \frac{Q}{\left[ (R^2 - Q^3)^{1/2} + |R| \right]^{1/3}} \right\} - \frac{A}{3}, \quad (\text{A.2})$$

- if  $Q^3 - R^2 \geq 0$ , three distinct real roots occur:

$$\begin{aligned} Z_1 &= -2\sqrt{Q} \cos\left(\frac{\theta}{3}\right) - \frac{A}{3}, Z_2 = -2\sqrt{Q} \cos\left(\frac{\theta+2\pi}{3}\right) - \frac{A}{3}, Z_3 = -2\sqrt{Q} \cos\left(\frac{\theta+4\pi}{3}\right) - \frac{A}{3}, \\ \theta &= \arccos\left(\frac{R}{Q^{3/2}}\right). \end{aligned} \quad (\text{A.3})$$

Given the fact that the middle root  $Z_2$  corresponds to an unstable state [22] we re-define:  $Z_1 = \text{MAX}(Z_1, Z_3)$  and  $Z_2 = \text{MIN}(Z_1, Z_3)$ . At this point, the following distinctions must be made:

- if this is a phase structure calculation, such as that required for Algorithm 1 in [Appendix F](#), the choice of the correct value of  $Z$  is made based on the known phase that is being solved for. If this is a liquid ( $\eta = L$ ) calculation, then  $Z = Z_2$ , while if this is a vapor ( $\eta = V$ ) calculation, then  $Z = Z_1$ . Note that all coefficients  $a_1-a_4$  need to be computed in the specific phase  $\eta$ ;
- if this is a direct calculation of the mixture compressibility using the single-fluid assumption, the choice is made based on the mixing Gibbs free energy [53]. By defining the quantity:

$$\frac{\Delta G_{\text{mix}}}{R_u T} = \sum_{i=1}^{N_s} X_i \left( \ln f_i(T, p, \mathbf{X}) \Big|_{Z=Z_2} - \ln f_i(T, p, \mathbf{X}) \Big|_{Z=Z_1} \right). \quad (\text{A.4})$$

Where  $f_i$  are the species fugacities calculated using their respective fugacity coefficient in Eq. [\(C.10\)](#), using either the liquid or the vapor compressibility, wherever it is required in the formulas. If  $\Delta G_{\text{mix}}/R_u T \geq 0$ , the vapor solution is chosen:  $Z = Z_1$  and the mixture is considered in the vapor state, otherwise, the liquid solution is chosen:  $Z = Z_2$  and the mixture is considered in the liquid state. This means that the mixture is always going to be made of a single phase and no VLE is possible to predict with this approach.

## Appendix B. Physical meaning of the “frozen” VLE assumption

In this appendix, we provide some details regarding the meaning of the “frozen” VLE assumption. First we begin with the derivative of the mixture density with respect to the temperature. Starting from Eq. [\(3.19\)](#) and using the fact that by assumption  $(\partial \beta / \partial T)_{p,\mathbf{X}} = (\partial M^V / \partial T)_{p,\mathbf{X}} = (\partial M^L / \partial T)_{p,\mathbf{X}} = 0$  one obtains the following:

$$\left( \frac{\partial \rho}{\partial T} \right)_{p,\mathbf{X}} = \frac{\rho^2}{M} \left[ \frac{\beta}{\rho^{V^2}} M^V \left( \frac{\partial \rho^V}{\partial T} \right)_{p,\mathbf{X}} + \frac{1-\beta}{\rho^{L^2}} M^L \left( \frac{\partial \rho^L}{\partial T} \right)_{p,\mathbf{X}} \right]. \quad (\text{B.1})$$

Note that it is not possible to completely separate the liquid portion from the vapor portion (thus writing the derivative in the form  $\Sigma = \beta \Sigma^V + (1-\beta) \Sigma^L$ ) because of  $\rho$  as in Eq. [\(3.4\)](#). As a result, an intrinsic non-linearity remains between the two phases for this specific term.

Next, we consider the specific heat at constant pressure. Starting from Eq. [\(3.8\)](#) and applying the frozen VLE conditions gives:

$$c_p = \beta \left( \frac{\partial E^V}{\partial T} \right)_{p,\mathbf{X}} + (1-\beta) \left( \frac{\partial E^L}{\partial T} \right)_{p,\mathbf{X}} - \frac{pM}{\rho^2} \left( \frac{\partial \rho}{\partial T} \right)_{p,\mathbf{X}}. \quad (\text{B.2})$$

Using the result of Eq. [\(B.1\)](#) and rearranging, one can easily verify that it gives  $c_p = \beta c_p^V + (1-\beta) c_p^L$ , i.e. exactly the approach used in [\[56\]](#). Using analogous concepts, the isothermal compressibility and the isobaric expansivity are obtained in the frozen VLE regime:

$$\alpha_p = -\frac{\rho}{M} \left[ \frac{\beta}{\rho^{V^2}} M^V \left( \frac{\partial \rho^V}{\partial T} \right)_{p,\mathbf{X}} + \frac{1-\beta}{\rho^{L^2}} M^L \left( \frac{\partial \rho^L}{\partial T} \right)_{p,\mathbf{X}} \right]. \quad (\text{B.3})$$

$$\kappa_T = \frac{\rho}{M} \left[ \frac{\beta}{\rho^{V^2}} M^V \left( \frac{\partial \rho^V}{\partial p} \right)_{T,\mathbf{X}} + \frac{1-\beta}{\rho^{L^2}} M^L \left( \frac{\partial \rho^L}{\partial p} \right)_{T,\mathbf{X}} \right]. \quad (\text{B.4})$$

Next, the isentropic compressibility is still computed with Eq. [\(C.9\)](#) and the speed of sound with Eq. [\(2.4\)](#). Note that a lot of non-linearities are retained even with the frozen assumption. This is mainly due to the density factor that pre-multiplies the terms representing each phase separately.

It is finally interesting to determine further insights on the speed of sound, and particularly on the way it is approximated with the classical Wood’s equation [\[83\]](#). First, Eq. [\(B.3\)](#) and Eq. [\(B.4\)](#) need to be further simplified and forced to be represented by a pure linear composition between the terms in each phase. To do so, we have to imagine to decompose the density factor and eliminate the non-linear

terms. Note this is not possible explicitly (easy to verify) and therefore this represents a strong assumption. In such a case, the above quantities become:

$$\alpha_p \approx - \left[ \frac{\beta}{\rho^V} \left( \frac{\partial \rho^V}{\partial T} \right)_{p,\mathbf{x}} + \frac{1-\beta}{\rho^L} \left( \frac{\partial \rho^L}{\partial T} \right)_{p,\mathbf{x}} \right] = \beta \alpha_p^V + (1-\beta) \alpha_p^L. \quad (\text{B.5})$$

$$\kappa_T \approx \left[ \frac{\beta}{\rho^V} \left( \frac{\partial \rho^V}{\partial p} \right)_{T,\mathbf{x}} + \frac{1-\beta}{\rho^L} \left( \frac{\partial \rho^L}{\partial p} \right)_{T,\mathbf{x}} \right] = \beta \kappa_T^V + (1-\beta) \kappa_T^L. \quad (\text{B.6})$$

Next, application of Eq. (C.9) gives:

$$\kappa_S = \beta \kappa_T^V + (1-\beta) \kappa_T^L - \frac{T}{\rho} \frac{\beta^2 \alpha_p^{V,2} + (1-\beta)^2 \alpha_p^{L,2} + 2\beta(1-\beta) \alpha_p^V \alpha_p^L}{\beta c_p^V + (1-\beta) c_p^L}. \quad (\text{B.7})$$

Elimination of all non-linear and cross terms between the phases, forces to employ the additional strong assumption:

$$\frac{T}{\rho} \frac{\beta^2 \alpha_p^{V,2} + (1-\beta)^2 \alpha_p^{L,2} + 2\beta(1-\beta) \alpha_p^V \alpha_p^L}{\beta c_p^V + (1-\beta) c_p^L} \approx T \left[ \beta \frac{\alpha_p^{V,2}}{\rho^V c_p^V} + (1-\beta) \frac{\alpha_p^{L,2}}{\rho^L c_p^L} \right],$$

now plugging the above result into Eq. (B.7) and rearranging:

$$\kappa_S = \underbrace{\beta \left( \kappa_T^V - \frac{T}{\rho^V} \frac{\alpha_p^{V,2}}{c_p^V} \right)}_{\kappa_S^V = 1/(\rho^V c^{V,2})} + (1-\beta) \underbrace{\left( \kappa_T^L - \frac{T}{\rho^L} \frac{\alpha_p^{L,2}}{c_p^L} \right)}_{\kappa_S^L = 1/(\rho^L c^{L,2})} = \beta \kappa_S^V + (1-\beta) \kappa_S^L = \frac{\beta}{\rho^V c^{V,2}} + \frac{1-\beta}{\rho^L c^{L,2}}. \quad (\text{B.8})$$

Hence, using Eq. (C.9), the following result is obtained:

$$c^2 = \frac{1}{\rho \left( \frac{\beta}{\rho^V c^{V,2}} + \frac{1-\beta}{\rho^L c^{L,2}} \right)}. \quad (\text{B.9})$$

which is the Wood's formula [83]. With the all discussion above, the following conclusions can be drawn:

- the frozen VLE assumption still retains some important non-linearities between the phases. Not all the quantities can be written in the linear form  $\Sigma = \beta \Sigma^V + (1-\beta) \Sigma^L$ . This is especially true for the speed of sound;
- if the frozen speed of sound is further simplified by eliminating all non-linear terms and forcing all the intermediate quantities to behave only linearly, the Wood's equation is retrieved. In these conditions, the only information about VLE is encapsulated in the values of  $\beta$ ,  $x_i$  and  $y_i$ . Hence, there is no surprise about the poor agreement that this correlation is known to exhibit [20].

## Appendix C. Single-phase thermodynamics mathematical details

$$\frac{\Delta E}{R_u T} = - \int_0^\rho T \left( \frac{\partial Z}{\partial T} \right)_{\rho,\mathbf{x}} \frac{d\rho}{\rho}, \quad (\text{C.1})$$

$$\frac{\Delta H}{R_u T} = \frac{\Delta E}{R_u T} + (Z-1), \quad (\text{C.2})$$

$$\frac{\Delta S}{R_u} = \int_0^\rho \left[ -T \left( \frac{\partial Z}{\partial T} \right)_{\rho,\mathbf{x}} - (Z-1) \right] \frac{d\rho}{\rho} + \ln Z = \frac{\Delta E}{R_u T} - \int_0^\rho (Z-1) \frac{d\rho}{\rho} + \ln Z, \quad (\text{C.3})$$

$$\frac{\Delta G}{R_u T} = \int_0^\rho \left( \frac{Z-1}{\rho} \right) d\rho + (Z-1) - \ln Z = \frac{\Delta H}{R_u T} - \frac{\Delta S}{R_u}, \quad (\text{C.4})$$

$$\frac{\Delta A}{R_u T} = \int_0^\rho \left( \frac{Z-1}{\rho} \right) d\rho - \ln Z = \frac{\Delta G}{R_u T} - (Z-1). \quad (\text{C.5})$$

$$\frac{\Delta A_{TV}}{R_u T} = \int_0^\rho \left( \frac{Z-1}{\rho} \right) d\rho. \text{(Helmholtz energy dept. func. when } T \text{ and } V \text{ are maintained constant}) \quad (\text{C.6})$$

$$\Delta c_v = \left( \frac{\partial \Delta E}{\partial T} \right)_{\rho,\mathbf{x}}, \quad \Delta c_p = \left( \frac{\partial \Delta H}{\partial T} \right)_{\rho,\mathbf{x}} = \Delta c_v + \frac{TM}{\rho^2} \left( \frac{\frac{\partial p}{\partial T}}{\frac{\partial p}{\partial \rho}} \right)_{\rho,\mathbf{x}} - R_u. \quad (\text{C.7})$$

$$\alpha_p = -\frac{1}{\rho} \left( \frac{\partial \rho}{\partial T} \right)_{p,\mathbf{X}} = \frac{1}{\rho} \frac{\left( \frac{\partial p}{\partial T} \right)_{\rho,\mathbf{X}}}{\left( \frac{\partial p}{\partial \rho} \right)_{T,\mathbf{X}}}, \quad \kappa_T = \frac{1}{\rho \left( \frac{\partial p}{\partial \rho} \right)_{T,\mathbf{X}}},$$

↓

$$\text{using } \left( \frac{\partial \rho}{\partial T} \right)_{p,\mathbf{X}} \left( \frac{\partial T}{\partial \rho} \right)_{\rho,\mathbf{X}} \left( \frac{\partial p}{\partial \rho} \right)_{T,\mathbf{X}} = -1 \quad (\text{C.8})$$

$$\kappa_s = \kappa_T - \frac{T\alpha_p^2}{\rho c_p}. \quad (\text{C.9})$$

$$\ln \phi_i(T, p, \mathbf{X}) = \frac{1}{R_u T} \left( \frac{\partial N \Delta A_{T,V}}{\partial N_i} \right)_{T,\bar{V},\mathbf{N}_i} - \ln Z, \quad (\text{C.10})$$

## Appendix D. Multi-phase thermodynamics mathematical details

To illustrate how to obtain each term of Eq. (3.9), we derive step-by-step the temperature derivatives of Eq. (3.9). The pressure derivatives follow an analogous approach. The fugacities equality of Eq. (3.1) is rewritten in logarithmic form, for convenience, and both sides are derived with respect to temperature:

$$\left( \frac{\partial \ln f_i^L}{\partial T} \right)_{p,\mathbf{X}} - \left( \frac{\partial \ln f_i^V}{\partial T} \right)_{p,\mathbf{X}} = 0, \quad i = 1, \dots, N_s. \quad (\text{D.1})$$

Given the link between the fugacity and fugacity coefficient for each  $i$ -th species in the phase  $\eta$ :

$$f_i^\eta = \phi_i^\eta p \zeta_i \rightarrow \ln f_i^\eta = \ln \phi_i^\eta + \ln p + \ln \zeta_i,$$

for the liquid phase ( $\eta=L$ ,  $\zeta=\mathbf{x}$ ):  $x_i = l_i/(1-\beta) = (X_i - v_i)/(1-\beta)$ , hence:

$$\left( \frac{\partial \ln f_i^L}{\partial T} \right)_{p,\mathbf{X}} = \frac{\partial}{\partial T} (\ln \phi_i^L + \ln p + \ln(X_i - v_i) - \ln(1-\beta))_{p,\mathbf{X}} = \left( \frac{\partial \ln \phi_i^L}{\partial T} \right)_{p,\mathbf{X}} - \frac{1}{X_i - v_i} \left( \frac{\partial v_i}{\partial T} \right)_{p,\mathbf{X}} + \frac{1}{1-\beta} \left( \frac{\partial \beta}{\partial T} \right)_{p,\mathbf{X}} \quad (\text{D.2})$$

Using the direct link between  $\beta$  and  $v_i$  of Eq. (3.11):

$$\left( \frac{\partial \beta}{\partial T} \right)_{p,\mathbf{X}} = \frac{\partial}{\partial T} \left( \sum_{k=1}^{N_s} v_k \right)_{p,\mathbf{X}} = \sum_{k=1}^{N_s} \left( \frac{\partial v_k}{\partial T} \right)_{p,\mathbf{X}}. \quad (\text{D.3})$$

Finally, substituting Eq. (D.3) into Eq. (D.2) one obtains for the liquid phase:

$$\left( \frac{\partial \ln f_i^L}{\partial T} \right)_{p,\mathbf{X}} = \left( \frac{\partial \ln \phi_i^L}{\partial T} \right)_{p,\mathbf{X}} + \frac{1}{1-\beta} \sum_{k=1}^{N_s} \left[ 1 - \left( \frac{1-\beta}{X_i - v_i} \right) \delta_{ki} \right] \left( \frac{\partial v_k}{\partial T} \right)_{p,\mathbf{X}}. \quad (\text{D.4})$$

For each  $i = 1, \dots, N_s$ . Where  $\delta_{ki}$  is the Kronecker delta. With analogous steps, one obtains for the vapor phase ( $\eta=V$ ,  $\zeta=\mathbf{x}$ ):

$$\left( \frac{\partial \ln f_i^V}{\partial T} \right)_{p,\mathbf{X}} = \left( \frac{\partial \ln \phi_i^V}{\partial T} \right)_{p,\mathbf{X}} - \frac{1}{\beta} \sum_{k=1}^{N_s} \left[ 1 - \left( \frac{\beta}{v_i} \right) \delta_{ki} \right] \left( \frac{\partial v_k}{\partial T} \right)_{p,\mathbf{X}} \quad i = 1, \dots, N_s. \quad (\text{D.5})$$

Substituting Eqs. (D.4) and (D.5) into Eq. (D.1), using Eq. (3.10) and rearranging, the following intermediate result is obtained in the unknowns  $(\partial v_k / \partial T)_{p,\mathbf{X}}$ :

$$\frac{1}{\beta(1-\beta)} \sum_{k=1}^{N_s} \left( 1 - \delta_{ki} \frac{X_k}{y_k x_k} \right) \left( \frac{\partial v_k}{\partial T} \right)_{p,\mathbf{X}} = \left( \frac{\partial \ln \phi_i^V}{\partial T} \right)_{p,\mathbf{X}} - \left( \frac{\partial \ln \phi_i^L}{\partial T} \right)_{p,\mathbf{X}} \quad i = 1, \dots, N_s. \quad (\text{D.6})$$

In addition, using the dependency between  $v_i$ ,  $\beta$ ,  $x_i$ ,  $y_i$  of Eq. (3.10), the following derivatives can be also obtained:

$$\left( \frac{\partial y_i}{\partial T} \right)_{p,\mathbf{X},y_i} = \left( \frac{\partial v_i / \beta}{\partial T} \right)_{p,\mathbf{X},y_i} = -\frac{y_i}{\beta} \sum_{k=1}^{N_s} \left( 1 - \frac{\delta_{ik}}{y_k} \right) \left( \frac{\partial v_k}{\partial T} \right)_{p,\mathbf{X}} \quad i = 1, \dots, N_s,$$

↓

Using Eq. (3.10) and Eq. (D.3)

$$\left( \frac{\partial x_i}{\partial T} \right)_{p,\mathbf{X},x_i} = \left( \frac{\partial (X_i - v_i) / (1-\beta)}{\partial T} \right)_{p,\mathbf{X},x_i} = \frac{x_i}{1-\beta} \sum_{k=1}^{N_s} \left( 1 - \frac{\delta_{ik}}{x_k} \right) \left( \frac{\partial v_k}{\partial T} \right)_{p,\mathbf{X}}.$$

↓

Using Eq. (3.10) and Eq. (D.3)

For each  $i = 1, \dots, N_s$ . Where  $\mathbf{y}_i = \{y_j | j = 1, \dots, N_s, j \neq i\}$  and  $\mathbf{x}_i = \{x_j | j = 1, \dots, N_s, j \neq i\}$  have been defined. For completeness, the temperature derivative of the  $K_i = y_i/x_i$  factors are also given. These can be easily constructed using Eq. (D.7) and Eq. (D.8):

$$\left( \frac{\partial K_i}{\partial T} \right)_{p,\mathbf{x}} = \frac{1}{\beta(1-\beta)x_i} \sum_{k=1}^{N_s} \left( \frac{\partial v_k}{\partial T} \right)_{p,\mathbf{x}} \left( \frac{X_i}{x_i} \delta_{ki} - y_k \right) \quad i = 1, \dots, N_s. \quad (\text{D.9})$$

Next, the derivatives of the fugacity coefficients in each phase appearing in Eq. (D.6) need to be addressed. Since for each  $i$ -th specie:  $\phi_i^V = \phi_i^V(T, p, \mathbf{y}(T, p, \mathbf{X}))$  and  $\phi_i^L = \phi_i^L(T, p, \mathbf{x}(T, p, \mathbf{X}))$ , using the total differential for each quantity (in logarithmic form) one obtains the “total” partial derivative of the fugacity coefficient with respect to temperature, at constant pressure:

$$\left( \frac{\partial \ln \phi_i^V}{\partial T} \right)_{p,\mathbf{x}} = \left( \frac{\partial \ln \phi_i^V}{\partial T} \right)_{p,\mathbf{x},\mathbf{y}} + \sum_{k=1}^{N_s} \left( \frac{\partial \ln \phi_i^V}{\partial y_k} \right)_{T,p,\mathbf{x},\mathbf{y}_k} \left( \frac{\partial y_k}{\partial T} \right)_{p,\mathbf{x},\mathbf{y}_k} \quad i = 1, \dots, N_s, \quad (\text{D.10})$$

$$\left( \frac{\partial \ln \phi_i^L}{\partial T} \right)_{p,\mathbf{x}} = \left( \frac{\partial \ln \phi_i^L}{\partial T} \right)_{p,\mathbf{x},\mathbf{x}} + \sum_{k=1}^{N_s} \left( \frac{\partial \ln \phi_i^L}{\partial x_k} \right)_{T,p,\mathbf{x},\mathbf{x}_k} \left( \frac{\partial x_k}{\partial T} \right)_{p,\mathbf{x},\mathbf{x}_k} \quad i = 1, \dots, N_s. \quad (\text{D.11})$$

The above derivatives are composed of two terms, one “frozen” part, which considers the phase composition fixed as the temperature is varied and the second that takes into account this variation. By taking the difference between Eq. (D.10) and Eq. (D.11), and substituting it into Eq. (D.6) and rearranging, the following formula is obtained:

$$\begin{aligned} & \sum_{k=1}^{N_s} \left\{ \left( 1 - \delta_{ki} \frac{X_k}{y_k x_k} \right) \right. \\ & \left. + \beta(1-\beta) \sum_{j=1}^{N_s} \left[ \frac{y_j}{\beta} \left( \frac{\partial \ln \phi_i^V}{\partial y_j} \right)_{T,p,\mathbf{x},\mathbf{y}_j} \left( 1 - \frac{\delta_{kj}}{y_j} \right) + \frac{x_j}{1-\beta} \left( \frac{\partial \ln \phi_i^L}{\partial x_j} \right)_{T,p,\mathbf{x},\mathbf{x}_j} \left( 1 - \frac{\delta_{jk}}{x_j} \right) \right] \right\} \left( \frac{\partial v_k}{\partial T} \right)_{p,\mathbf{x}} = \\ & = \beta(1-\beta) \left[ \left( \frac{\partial \ln \phi_i^V}{\partial T} \right)_{p,\mathbf{x},\mathbf{y}} - \left( \frac{\partial \ln \phi_i^L}{\partial T} \right)_{p,\mathbf{x},\mathbf{x}} \right] \quad i = 1, \dots, N_s. \end{aligned} \quad (\text{D.12})$$

If analogous steps are repeated for the derivatives with respect to pressure, the following results are obtained

$$\left( \frac{\partial \beta}{\partial p} \right)_{T,\mathbf{x}} = \sum_{k=1}^{N_s} \left( \frac{\partial v_k}{\partial p} \right)_{T,\mathbf{x}}, \quad (\text{D.13})$$

$$\left( \frac{\partial y_i}{\partial p} \right)_{T,\mathbf{x},\mathbf{y}_i} = -\frac{y_i}{\beta} \sum_{k=1}^{N_s} \left( 1 - \frac{\delta_{ik}}{y_k} \right) \left( \frac{\partial v_k}{\partial p} \right)_{T,\mathbf{x}} \quad i = 1, \dots, N_s, \quad (\text{D.14})$$

$$\left( \frac{\partial x_i}{\partial p} \right)_{T,\mathbf{x},\mathbf{x}_i} = \frac{x_i}{1-\beta} \sum_{k=1}^{N_s} \left( 1 - \frac{\delta_{ik}}{x_k} \right) \left( \frac{\partial v_k}{\partial p} \right)_{T,\mathbf{x}} \quad i = 1, \dots, N_s, \quad (\text{D.15})$$

$$\left( \frac{\partial K_i}{\partial p} \right)_{T,\mathbf{x}} = \frac{1}{\beta(1-\beta)x_i} \sum_{k=1}^{N_s} \left( \frac{\partial v_k}{\partial p} \right)_{T,\mathbf{x}} \left( \frac{X_i}{x_i} \delta_{ki} - y_k \right) \quad i = 1, \dots, N_s. \quad (\text{D.16})$$

$$\begin{aligned} & \sum_{k=1}^{N_s} \left\{ \left( 1 - \delta_{ki} \frac{X_k}{y_k x_k} \right) \right. \\ & \left. + \beta(1-\beta) \sum_{j=1}^{N_s} \left[ \frac{y_j}{\beta} \left( \frac{\partial \ln \phi_i^V}{\partial y_j} \right)_{T,p,\mathbf{x},\mathbf{y}_j} \left( 1 - \frac{\delta_{kj}}{y_j} \right) + \frac{x_j}{1-\beta} \left( \frac{\partial \ln \phi_i^L}{\partial x_j} \right)_{T,p,\mathbf{x},\mathbf{x}_j} \left( 1 - \frac{\delta_{jk}}{x_j} \right) \right] \right\} \left( \frac{\partial v_k}{\partial p} \right)_{T,\mathbf{x}} = \\ & = \beta(1-\beta) \left[ \left( \frac{\partial \ln \phi_i^V}{\partial p} \right)_{T,\mathbf{x},\mathbf{y}} - \left( \frac{\partial \ln \phi_i^L}{\partial p} \right)_{T,\mathbf{x},\mathbf{x}} \right] \quad i = 1, \dots, N_s. \end{aligned} \quad (\text{D.17})$$

By looking at Eq. (D.12) and Eq. (D.17) one immediately realizes that both linear systems can be written in the following compact form:  $\mathbf{A}\chi_T = \mathbf{b}_T$  and  $\mathbf{A}\chi_p = \mathbf{b}_p$ , where  $\mathbf{A}_{ik}$ ,  $b_{T,i}$ ,  $b_{p,i}$ ,  $\chi_{T,k}$  and  $\chi_{p,k}$  are those given in Eqs. (3.14)–(3.18). Additional useful relations are given below:

$$\begin{aligned} & \left( \frac{\partial M^V}{\partial T} \right)_{p,\mathbf{x}} = \frac{\partial}{\partial T} \left( \sum_{k=1}^{N_s} y_k M_k \right)_{p,\mathbf{x}} \stackrel{\text{Using Eq. (3.10)}}{\downarrow} \frac{1}{\beta^2} \sum_{k=1}^{N_s} \left[ \left( \frac{\partial v_k}{\partial T} \right)_{p,\mathbf{x}} - v_k \left( \frac{\partial \beta}{\partial T} \right)_{p,\mathbf{x}} \right] M_k, \\ & \quad (\text{D.18}) \end{aligned}$$

$$\left( \frac{\partial M^V}{\partial p} \right)_{T,\mathbf{x}} = \frac{\partial}{\partial p} \left( \sum_{k=1}^{N_s} y_k M_k \right)_{T,\mathbf{x}} = \frac{1}{\beta^2} \sum_{k=1}^{N_s} \left[ \left( \frac{\partial v_k}{\partial p} \right)_{T,\mathbf{x}} - \nu_k \left( \frac{\partial \beta}{\partial p} \right)_{T,\mathbf{x}} \right] M_k \quad (\text{D.19})$$

$$\left( \frac{\partial M^L}{\partial T} \right)_{p,\mathbf{x}} = \frac{\partial}{\partial T} \left( \sum_{k=1}^{N_s} x_k M_k \right)_{p,\mathbf{x}} = \frac{1}{(1-\beta)^2} \sum_{k=1}^{N_s} \left[ (X_k - \nu_k) \left( \frac{\partial \beta}{\partial T} \right)_{p,\mathbf{x}} - \left( \frac{\partial v_k}{\partial T} \right)_{p,\mathbf{x}} (1-\beta) \right] M_k, \quad (\text{D.20})$$

$$\left( \frac{\partial M^L}{\partial p} \right)_{T,\mathbf{x}} = \frac{\partial}{\partial p} \left( \sum_{k=1}^{N_s} x_k M_k \right)_{T,\mathbf{x}} = \frac{1}{(1-\beta)^2} \sum_{k=1}^{N_s} \left[ (X_k - \nu_k) \left( \frac{\partial \beta}{\partial p} \right)_{T,\mathbf{x}} - \left( \frac{\partial v_k}{\partial p} \right)_{T,\mathbf{x}} (1-\beta) \right] M_k. \quad (\text{D.21})$$

Additional mixture, as well as phase-related derivatives are given below. The derivative of the pressure with respect to temperature using the link between Eq. (3.19) and Eq. (3.20):

$$\left( \frac{\partial \rho}{\partial T} \right)_{p,\mathbf{x}} \left( \frac{\partial T}{\partial p} \right)_{\rho,\mathbf{x}} \left( \frac{\partial p}{\partial \rho} \right)_{T,\mathbf{x}} = -1 \quad \rightarrow \quad \left( \frac{\partial p}{\partial T} \right)_{\rho,\mathbf{x}} = - \frac{\left( \frac{\partial \rho}{\partial T} \right)_{p,\mathbf{x}}}{\left( \frac{\partial \rho}{\partial p} \right)_{T,\mathbf{x}}}. \quad (\text{D.22})$$

Eq. (3.19), Eq. (3.20) and Eq. (D.22) require the knowledge of the derivatives of  $\rho^V = \rho^V(T, p, \mathbf{y}(T, p, \mathbf{X}))$  and  $\rho^L = \rho^L(T, p, \mathbf{x}(T, p, \mathbf{X}))$ . In short notation, for the generic phase  $\eta = (L \text{ or } V)$  with molar composition  $\zeta$  one can write the total differential of  $\rho^\eta = \rho^\eta(T, p, \zeta(T, p, \mathbf{X}))$ :

$$d\rho^\eta = \left( \frac{\partial \rho^\eta}{\partial T} \right)_{p,\mathbf{x},\zeta} dT + \left( \frac{\partial \rho^\eta}{\partial p} \right)_{T,\mathbf{x},\zeta} dp + \sum_{k=1}^{N_s} \left( \frac{\partial \rho^\eta}{\partial \zeta_k} \right)_{T,p,\mathbf{x},\zeta_k} d\zeta_k, \quad (\text{D.23})$$

where  $\zeta_k = \{\zeta_i | i = 1, \dots, N_s, i \neq k\}$ . From Eq. (D.23) the “total” derivatives with respect to temperature and pressure follows:

$$\left( \frac{\partial \rho^\eta}{\partial T} \right)_{p,\mathbf{x}} = \left( \frac{\partial \rho^\eta}{\partial T} \right)_{p,\mathbf{x},\zeta} + \sum_{k=1}^{N_s} \left( \frac{\partial \rho^\eta}{\partial \zeta_k} \right)_{T,p,\mathbf{x},\zeta_k} \left( \frac{\partial \zeta_k}{\partial T} \right)_{p,\mathbf{x},\zeta_k}, \quad (\text{D.24})$$

$$\left( \frac{\partial \rho^\eta}{\partial p} \right)_{T,\mathbf{x}} = \left( \frac{\partial \rho^\eta}{\partial p} \right)_{T,\mathbf{x},\zeta} + \sum_{k=1}^{N_s} \left( \frac{\partial \rho^\eta}{\partial \zeta_k} \right)_{T,p,\mathbf{x},\zeta_k} \left( \frac{\partial \zeta_k}{\partial p} \right)_{T,\mathbf{x},\zeta_k}. \quad (\text{D.25})$$

Eqs. (D.24) and (D.25) require the additional derivative of the phase density with respect to the phase mole fraction. This is obtained by applying the general form of the EoS as in Eq. (2.2):

$$\left( \frac{\partial \rho^\eta}{\partial \zeta_k} \right)_{T,p,\mathbf{x},\zeta_k} = \frac{M_k Z^\eta - M^\eta \left( \frac{\partial Z^\eta}{\partial \zeta_k} \right)_{T,p,\zeta_k}}{\frac{p}{R_u T} (Z^\eta)^2}.$$

↓

Use  $\rho^\eta = p M^\eta / Z^\eta R_u T$  and  $M^\eta = \sum_{k=1}^{N_s} \zeta_k M_k$

(D.26)

In the above, the (frozen) derivative  $\left( \frac{\partial Z^\eta}{\partial \zeta_k} \right)_{T,p,\zeta_k}$  requires a specific EoS model as well. Given the form of the EoS assumed to be explicit in pressure as in Eq. (2.1), a note must be made on the phase pressure/density/temperature derivatives. Particularly one can compute (without loss of generality):

$$\left( \frac{\partial \rho^\eta}{\partial p} \right)_{T,\mathbf{x},\zeta} = \frac{1}{\left( \frac{\partial p}{\partial \rho^\eta} \right)_{T,\mathbf{x},\zeta}}, \quad \left( \frac{\partial \rho^\eta}{\partial T} \right)_{p,\mathbf{x},\zeta} = - \frac{\left( \frac{\partial p}{\partial T} \right)_{\rho^\eta,\mathbf{x},\zeta}}{\left( \frac{\partial p}{\partial \rho^\eta} \right)_{T,\mathbf{x},\zeta}},$$
(D.27)

$$\text{Using } \left( \frac{\partial \rho^\eta}{\partial T} \right)_{p,\mathbf{x},\zeta} \left( \frac{\partial T}{\partial p} \right)_{\rho^\eta,\mathbf{x},\zeta} \left( \frac{\partial p}{\partial \rho^\eta} \right)_{T,\mathbf{x},\zeta} = -1$$
(D.27)

where now  $\left( \frac{\partial p}{\partial \rho^\eta} \right)_{T,\mathbf{x},\zeta}$  and  $\left( \frac{\partial p}{\partial T} \right)_{\rho^\eta,\mathbf{x},\zeta}$  can be directly computed from the EoS model.

Next, the derivatives of the phase compressibilities are obtained. Using the general form of  $Z^\eta = Z^\eta(T, p, \zeta(T, p, \mathbf{X}))$  and writing the total differential one gets:

$$\left( \frac{\partial Z^\eta}{\partial T} \right)_{p,\mathbf{x}} = \left( \frac{\partial Z^\eta}{\partial T} \right)_{p,\mathbf{x},\zeta} + \sum_{k=1}^{N_s} \left( \frac{\partial Z^\eta}{\partial \zeta_k} \right)_{T,p,\mathbf{x},\zeta_k} \left( \frac{\partial \zeta_k}{\partial T} \right)_{p,\mathbf{x},\zeta_k},$$
(D.28)

$$\left( \frac{\partial Z^\eta}{\partial p} \right)_{T,\mathbf{x}} = \left( \frac{\partial Z^\eta}{\partial p} \right)_{T,\mathbf{x},\zeta} + \sum_{k=1}^{N_s} \left( \frac{\partial Z^\eta}{\partial \zeta_k} \right)_{T,p,\mathbf{x},\zeta_k} \left( \frac{\partial \zeta_k}{\partial p} \right)_{T,\mathbf{x},\zeta_k}, \quad (\text{D.29})$$

where  $(\partial Z^\eta / \partial T)_{p,\mathbf{x},\zeta}$  and  $(\partial Z^\eta / \partial p)_{T,\mathbf{x},\zeta}$  can be also computed from the EoS model.

On the other hand the mixture compressibility derivatives are obtained by differentiating Eq. (2.1):

Using  $Z = pM/\rho R_u T$

$$\left( \frac{\partial Z}{\partial T} \right)_{p,\mathbf{x}} \downarrow = \frac{pM}{R_u} \frac{\partial}{\partial T} \left( \frac{1}{\rho T} \right)_{p,\mathbf{x}} = \frac{pM}{R_u} \frac{\left[ \rho - T \left( \frac{\partial \rho}{\partial T} \right)_{p,\mathbf{x}} \right]}{(\rho T)^2}, \quad (\text{D.30})$$

$$\left( \frac{\partial Z}{\partial p} \right)_{T,\mathbf{x}} = \frac{M}{R_u T} \frac{\partial}{\partial p} \left( \frac{p}{\rho} \right)_{T,\mathbf{x}} = \frac{M}{R_u T} \left[ \rho - p \left( \frac{\partial \rho}{\partial p} \right)_{T,\mathbf{x}} \right]. \quad (\text{D.31})$$

Note that the form of Eqs. (D.30) and (D.31) holds for a single phase mixture identically (that is can be used in single phase conditions too).

Finally, the last important variations to compute are the phases internal energy derivatives that appear in Eq. (3.21) and Eq. (3.22). Given that  $E^\eta = E^\eta(T, p, \zeta(T, p, \mathbf{x}))$ , using again the total differential, the following phase related derivatives are obtained:

$$\left( \frac{\partial E^\eta}{\partial T} \right)_{p,\mathbf{x}} = \left( \frac{\partial E^\eta}{\partial T} \right)_{p,\mathbf{x},\zeta} + \sum_{k=1}^{N_s} \left( \frac{\partial E^\eta}{\partial \zeta_k} \right)_{T,p,\mathbf{x},\zeta_k} \left( \frac{\partial \zeta_k}{\partial T} \right)_{p,\mathbf{x},\zeta_k}, \quad (\text{D.32})$$

$$\left( \frac{\partial E^\eta}{\partial p} \right)_{T,\mathbf{x}} = \left( \frac{\partial E^\eta}{\partial p} \right)_{T,\mathbf{x},\zeta} + \sum_{k=1}^{N_s} \left( \frac{\partial E^\eta}{\partial \zeta_k} \right)_{T,p,\mathbf{x},\zeta_k} \left( \frac{\partial \zeta_k}{\partial p} \right)_{T,\mathbf{x},\zeta_k}, \quad (\text{D.33})$$

where:

$$\left( \frac{\partial E^\eta}{\partial \zeta_k} \right)_{T,p,\mathbf{x},\zeta_k} = \frac{\partial}{\partial \zeta_k} (E^{\eta,ig} + \Delta E^\eta)_{T,p,\mathbf{x},\zeta_k} = \frac{\partial}{\partial \zeta_k} \left( \sum_{j=1}^{N_s} \zeta_j e_j^{ig} \right)_{T,p,\mathbf{x},\zeta_k} + \left( \frac{\partial \Delta E^\eta}{\partial \zeta_k} \right)_{T,p,\mathbf{x},\zeta_k} = e_k^{ig} + \left( \frac{\partial \Delta E^\eta}{\partial \zeta_k} \right)_{T,p,\mathbf{x},\zeta_k}. \quad (\text{D.34})$$

$$\left( \frac{\partial E^\eta}{\partial T} \right)_{p,\mathbf{x},\zeta} = \frac{\partial}{\partial T} (E^{\eta,ig} + \Delta E^\eta)_{p,\mathbf{x},\zeta} = \frac{\partial}{\partial T} \left( \sum_{j=1}^{N_s} \zeta_j e_j^{ig} \right)_{T,p,\mathbf{x},\zeta} + \left( \frac{\partial \Delta E^\eta}{\partial T} \right)_{p,\mathbf{x},\zeta} = c_v^{\eta,ig} + \left( \frac{\partial \Delta E^\eta}{\partial T} \right)_{p,\mathbf{x},\zeta}. \quad (\text{D.35})$$

$$\left( \frac{\partial E^\eta}{\partial p} \right)_{T,\mathbf{x},\zeta} = \frac{\partial}{\partial p} (E^{\eta,ig} + \Delta E^\eta)_{T,\mathbf{x},\zeta} = \sum_{j=1}^{N_s} \zeta_j \left( \frac{de_j^{ig}}{dp} \right) + \left( \frac{\partial \Delta E^\eta}{\partial p} \right)_{T,\mathbf{x},\zeta} = \left( \frac{\partial \Delta E^\eta}{\partial p} \right)_{T,\mathbf{x},\zeta}. \quad (\text{D.36})$$

Where  $(\partial \Delta E^\eta / \partial T)_{p,\mathbf{x},\zeta}$ ,  $(\partial \Delta E^\eta / \partial p)_{T,\mathbf{x},\zeta}$  and  $(\partial \Delta E^\eta / \partial \zeta_k)_{T,p,\mathbf{x},\zeta_k}$  are again computed with an EoS model. In the above,  $c_{v,j}^{ig}$  and  $e_j^{ig}$  have been used to denote the  $j$ -th species IG specific heat at constant volume and internal energy, respectively, while  $c_v^{\eta,ig}$  indicated the mixture IG specific heat at constant volume in the phase  $\eta$ .

## Appendix E. Multi-phase partial molar quantities mathematical details

We first recall the starting point of Eq. (3.27) written for both phases:

$$\left( \frac{\partial \bar{V}^V}{\partial N_i} \right)_{T,p,\mathbf{N}_i} = \sum_{k=1}^{N_s} \left( \frac{\partial \bar{V}^V}{\partial N_k^V} \right)_{T,p,\mathbf{N}_k^V} \left( \frac{\partial N_k^V}{\partial N_i} \right)_{T,p,\mathbf{N}_k^V, \mathbf{N}_i} \quad i = 1, \dots, N_s, \quad (\text{E.1})$$

$$\left( \frac{\partial \bar{V}^L}{\partial N_i} \right)_{T,p,\mathbf{N}_i} = \sum_{k=1}^{N_s} \left( \frac{\partial \bar{V}^L}{\partial N_k^L} \right)_{T,p,\mathbf{N}_k^L} \left( \frac{\partial N_k^L}{\partial N_i} \right)_{T,p,\mathbf{N}_k^L, \mathbf{N}_i} \quad i = 1, \dots, N_s. \quad (\text{E.2})$$

Regarding the first term in the sum, using the fact that  $p\bar{V}^\eta = \sigma Z^\eta R_u T$  (with  $\sigma$  defined in Eq. (3.25)), one can write for both phases:

$$\left( \frac{\partial \bar{V}^V}{\partial N_k^V} \right)_{T,p,\mathbf{N}_k^V} = \frac{R_u T}{p} \frac{\partial}{\partial N_k^V} (N^V Z^V)_{T,p,\mathbf{N}_k^V} = \frac{R_u T}{p} \left[ Z^V + N^V \left( \frac{\partial Z^V}{\partial N_k^V} \right)_{T,p,\mathbf{N}_k^V} \right], \quad (\text{E.3})$$

$$\left( \frac{\partial \bar{V}^L}{\partial N_k^L} \right)_{T,p,\mathbf{N}_k^L} = \frac{R_u T}{p} \frac{\partial}{\partial N_k^L} (N^L Z^L)_{T,p,\mathbf{N}_k^L} = \frac{R_u T}{p} \left[ Z^L + N^L \left( \frac{\partial Z^L}{\partial N_k^L} \right)_{T,p,\mathbf{N}_k^L} \right]. \quad (\text{E.4})$$

To proceed further, a conversion between a mole based derivative to a mole fraction based derivative is required. The reason for this is that some numerical simulation tools are based on mass/mole fractions and therefore having the formulas based on these is more convenient. The link between the two quantities is given by the following identity (easy to verify):

$$\left( \frac{\partial(\cdot)}{\partial N_j} \right)_{T,p,\mathbf{N}_j} = \sum_{k=1}^{N_s} \left( \frac{\partial(\cdot)}{\partial X_k} \right)_{T,p,\mathbf{x}_k} \frac{\delta_{kj} - X_k}{N}. \quad (\text{E.5})$$

After applying Eq. (E.5) to the compressibility derivatives of Eq. (E.3) and Eq. (E.4) one can easily get their modified version:

$$\left( \frac{\partial \bar{V}^V}{\partial N_k^V} \right)_{T,p,\mathbf{N}_k^V} = \frac{R_u T}{p} \left[ Z^V + \sum_{j=1}^{N_s} \left( \frac{\partial Z^V}{\partial y_j} \right)_{T,p,\mathbf{y}_j} (\delta_{jk} - y_j) \right], \quad (\text{E.6})$$

$$\left( \frac{\partial \bar{V}^L}{\partial N_k^L} \right)_{T,p,\mathbf{N}_k^L} = \frac{R_u T}{p} \left[ Z^L + \sum_{j=1}^{N_s} \left( \frac{\partial Z^L}{\partial x_j} \right)_{T,p,\mathbf{x}_j} (\delta_{jk} - x_j) \right]. \quad (\text{E.7})$$

Where both  $(\partial Z^V / \partial y_j)_{T,p,\mathbf{y}_j}$  and  $(\partial Z^V / \partial x_j)_{T,p,\mathbf{x}_j}$  can be now easily obtained from the EoS model. Next, the unknowns  $(\partial \sigma_k / \partial N_i)_{T,p,\sigma_k,\mathbf{N}_i}$  are derived. To begin, the equilibrium condition of Eq. (3.1) (in logarithmic form) and the continuity condition:  $N_k = N_k^L + N_k^V$ ,  $k = 1, \dots, N_s$  are differentiated with respect to the  $i$ -th species mole number:

$$\left( \frac{\partial \ln f_k^L}{\partial N_i} \right)_{T,p,\mathbf{N}_i} - \left( \frac{\partial \ln f_k^V}{\partial N_i} \right)_{T,p,\mathbf{N}_i} = 0 \quad i, k = 1, \dots, N_s, \quad (\text{E.8})$$

$$\left( \frac{\partial N_k^L}{\partial N_i} \right)_{T,p,\mathbf{N}_k^L,\mathbf{N}_i} + \left( \frac{\partial N_k^V}{\partial N_i} \right)_{T,p,\mathbf{N}_k^V,\mathbf{N}_i} = \left( \frac{\partial N_k}{\partial N_i} \right)_{T,p,\mathbf{N}_i} \quad i, k = 1, \dots, N_s. \quad (\text{E.9})$$

Since  $\ln f_k^\eta = \ln f_k^\eta(T, p, \sigma)$ , application of the total differential for both phases at constant  $T$  and  $p$  and its differentiation with respect to the  $i$ -th species mole number allows to rewrite Eq. (E.8) as:

$$\sum_{j=1}^{N_s} \left[ \left( \frac{\partial \ln f_k^L}{\partial N_j^L} \right)_{T,p,\mathbf{N}_j^L} \left( \frac{\partial N_j^L}{\partial N_i} \right)_{T,p,\mathbf{N}_j^L,\mathbf{N}_i} - \left( \frac{\partial \ln f_k^V}{\partial N_j^V} \right)_{T,p,\mathbf{N}_j^V} \left( \frac{\partial N_j^V}{\partial N_i} \right)_{T,p,\mathbf{N}_j^V,\mathbf{N}_i} \right] = 0 \quad i, k = 1, \dots, N_s. \quad (\text{E.10})$$

Conversion of the fugacity to its corresponding fugacity coefficient and application of Eq. (E.5) produces the following additional step:

$$\begin{aligned} \sum_{j=1}^{N_s} \left\{ \left[ \sum_{s=1}^{N_s} \left( \frac{\partial \ln \phi_k^L}{\partial x_s} \right)_{T,p,\mathbf{x}_s} \left( \frac{\delta_{sj} - x_s}{1 - \beta} \right) + \frac{1}{x_k} \frac{\delta_{kj} - x_k}{1 - \beta} \right] \left( \frac{\partial N_j^L}{\partial N_i} \right)_{T,p,\mathbf{N}_j^L,\mathbf{N}_i} \right. \\ \left. \left[ \sum_{s=1}^{N_s} \left( \frac{\partial \ln \phi_k^V}{\partial y_s} \right)_{T,p,\mathbf{y}_s} \left( \frac{\delta_{sj} - y_s}{\beta} \right) + \frac{1}{y_k} \frac{\delta_{kj} - y_k}{\beta} \right] \left( \frac{\partial N_j^V}{\partial N_i} \right)_{T,p,\mathbf{N}_j^V,\mathbf{N}_i} \right\} = 0 \quad i, k = 1, \dots, N_s. \end{aligned} \quad (\text{E.11})$$

Where the relations  $\beta = N^V/N$  and  $1 - \beta = N^L/N$  have been also used after multiplying both sides by  $N$ . Using Eq. (E.9) one can reduce the number of variables by expressing one set as a function of the other set. Without loss of generality, by expressing the derivatives of the liquid phase as a function of those in the vapor phase, one gets the following relationship:

$$\left( \frac{\partial N_k^L}{\partial N_i} \right)_{T,p,\mathbf{N}_k^L,\mathbf{N}_i} = \delta_{ki} - \left( \frac{\partial N_k^V}{\partial N_i} \right)_{T,p,\mathbf{N}_k^V,\mathbf{N}_i} \quad i, k = 1, \dots, N_s. \quad (\text{E.12})$$

Hence, using Eq. (E.12) into Eq. (E.11) and rearranging the final result  $\mathbf{C}\chi_N^{(i)} = \mathbf{b}_N^{(i)}$  is obtained where  $C_{kj}$ ,  $b_{N,k}^{(i)}$  and  $\chi_{N,j}^{(i)}$  have been given in Eqs. (3.29)–(3.31). The present linear system needs to be solved  $N_s$  times in the unknown vector  $\chi_N^{(i)}$ . Finally, for the partial molar enthalpy we start from its definition:

$$\begin{aligned}
h_i &= \left( \frac{\partial \bar{H}}{\partial N_i} \right)_{T,p,\mathbf{N}_i} = \left( \frac{\partial NH}{\partial N_i} \right)_{T,p,\mathbf{N}_i} = \left( \frac{\partial N \left( E + \frac{pM}{\rho} \right)}{\partial N_i} \right)_{T,p,\mathbf{N}_i} \stackrel{\overline{V} = NV = NM/\rho}{\downarrow} \left( \frac{\partial (\bar{E} + p\bar{V})}{\partial N_i} \right)_{T,p,\mathbf{N}_i} \\
&= p \left( \frac{\partial \bar{V}}{\partial N_i} \right)_{T,p,\mathbf{N}_i} + \left( \frac{\partial \bar{E}^V}{\partial N_i} \right)_{T,p,\mathbf{N}_i} + \left( \frac{\partial \bar{E}^L}{\partial N_i} \right)_{T,p,\mathbf{N}_i} \quad i = 1, \dots, N_s, \\
&\stackrel{\downarrow}{=} \bar{E} = N[\beta E^V + (1 - \beta)E^L] = N^V E^V + N^L E^L = \bar{E}^V + \bar{E}^L
\end{aligned}$$

$\bar{E} = N[\beta E^V + (1 - \beta) E^L] = N^V E^V + N^L E^L = \bar{E}^V + \bar{E}^L$  which leads to Eq. (3.32). In compact form, writing once again the total differential for  $\bar{E}^\eta = \bar{E}^\eta(T, p, \sigma)$  at constant  $T$  and  $p$  and using again Eq. (E.5) to convert to mole number to mole fraction derivative, the following result is obtained:

$$\left( \frac{\partial \bar{E}^V}{\partial N_i} \right)_{T,p,\mathbf{N}_i} = \sum_{k=1}^{N_s} \left\{ E^V + \sum_{s=1}^{N_s} \left[ \left( \frac{\partial E^V}{\partial y_k} \right)_{T,p,\mathbf{y}_k} (\delta_{sk} - y_s) \right] \right\} \left( \frac{\partial N_k^V}{\partial N_i} \right)_{T,p,\mathbf{N}_k^V, \mathbf{N}_i} \quad i = 1, \dots, N_s, \quad (\text{E.13})$$

$$\left( \frac{\partial \bar{E}^L}{\partial N_i} \right)_{T,p,\mathbf{N}_i} = \sum_{k=1}^{N_s} \left\{ E^L + \sum_{s=1}^{N_s} \left[ \left( \frac{\partial E^L}{\partial x_k} \right)_{T,p,x_k} (\delta_{sk} - x_s) \right] \right\} \left( \frac{\partial N_k^L}{\partial N_i} \right)_{T,p,\mathbf{N}_k^L,\mathbf{N}_i} \quad i = 1, \dots, N_s. \quad (\text{E.14})$$

Where the derivatives  $(\partial E^n / \partial \zeta_k)_{T,p,\zeta_k}$  are assumed to be available with the EoS model by applying Algorithm 5 and derivatives  $(\partial N_k^V / \partial N_i)_{T,p,N_k^V,N_i}$  and  $(\partial N_k^L / \partial N_i)_{T,p,N_k^L,N_i}$  correspond to  $\chi_N^{(i)}$  already computed with Eq. (3.28).

## Appendix F. Algorithms for the present thermodynamic model

**Algorithm 1.** generateVLstructure( $T, p, \xi, \eta$ )

- 1: **Inputs:**  $T, p, \zeta \leftarrow x$  if  $\eta = L$  or  $\zeta \leftarrow y$  if  $\eta = V$   
 2: **Compute phase molar mass:**  $M^\eta = M^\eta(\zeta)$  with  $M^\eta = \sum_{i=1}^{N_s} \zeta_i M_i$   
 3: **Compute phase compressibility:** solve  $Z^\eta = Z^\eta(T, p, \zeta, \eta)$  see [Appendix A](#)  
 4: **Compute phase density:**  $\rho^\eta = pM^\eta / Z^\eta R_t T$   
 5: **Compute phase energies:**  $[E^\eta, H^\eta, S^\eta, G^\eta, A^\eta] = [E^\eta, H^\eta, S^\eta, G^\eta, A^\eta](T, p, \zeta)$  using Eqs. (C.1)–(C.5)  
 6: **Compute phase fugacity coefficient:**  $\phi_i^\eta = \phi_i^\eta(T, p, \zeta)$   $i = 1, \dots, N_s$  using Eq. (C.10)  
 7: **Compute phase fugacity:**  $f_i^\eta = f_i^\eta(T, p, \zeta)$  using  $f_i^\eta = p\phi_i^\eta \zeta_i$   $i = 1, \dots, N_s$

**Algorithm 2.** solveTP( $T, p, \mathbf{X}$ )

- 1: **Inputs:**  $T, p, X$   
 2: **Solve VLE problem:**  $[\beta, \mathbf{x}, \mathbf{y}] = \text{VLE}(T, p, \mathbf{X})$  using Eqs. (3.6)–(3.7) (see [53, 54, 78])  
 3: **Obtain liquid mixture:**  $\text{CALL generateVLstructure}(T, p, \mathbf{x}, L)$  using Algorithm 1  
 4: **Obtain vapor mixture:**  $\text{CALL generateVLstructure}(T, p, \mathbf{y}, V)$  using Algorithm 1  
 5: **Compute mixture density:**  $\rho$  - Use Eq. (3.4)  
 6: **Compute mixture compressibility:**  $Z$  - Use Eq. (2.2) (Note  $M$  uses  $\mathbf{X}$  here computed using  $M = \sum_{i=1}^{N_s} X_i M_i$ )  
 7: **Compute mixture energies:**  $E$  - Use Eq. (3.5),  $H, S, G, A$  using their definitions (e.g.  $H = E + pM/\rho$ )

**Algorithm 3.** computeTPvariations( $T, p, \mathbf{X}, \beta, \mathbf{x}, \mathbf{y}$ )

- 1: **Inputs:**  $T, p, \mathbf{X}, \beta, \mathbf{x}, \mathbf{y}$   
 2: **Obtain liquid mixture:** CALL `generateVLstructure( $T, p, \mathbf{x}, L$ )` using Algorithm 1  
 3: **Obtain vapor mixture:** CALL `generateVLstructure( $T, p, \mathbf{y}, V$ )` using Algorithm 1  
 4: **Compute and store:**  $\left( \frac{\partial \ln \phi_i^V}{\partial y_j} \right)_{T, p, \mathbf{X}, \mathbf{y}_j}, \left( \frac{\partial \ln \phi_i^L}{\partial x_k} \right)_{T, p, \mathbf{X}, \mathbf{x}_k}, \left( \frac{\partial \ln \phi_i^V}{\partial T} \right)_{p, \mathbf{X}, \mathbf{y}}, \left( \frac{\partial \ln \phi_i^L}{\partial T} \right)_{p, \mathbf{X}, \mathbf{x}}, \left( \frac{\partial \ln \phi_i^V}{\partial p} \right)_{T, \mathbf{X}, \mathbf{y}}, \left( \frac{\partial \ln \phi_i^L}{\partial p} \right)_{T, \mathbf{X}, \mathbf{x}}$ , with an EoS  
 5: **Compute and store:**  $A_{ik}, b_{T,i}, b_{p,i}$  using Eqs. (3.14)–(3.16)  
 6: **Compute and store:**  $\chi_T, \chi_p$  by inverting Eq. (3.12) and Eq. (3.13), respectively  
 7: **Compute:** all quantities in Eq. (3.9) using Eq. (D.3), Eq. (D.7), Eq. (D.8), Eqs. (D.13)–(D.15)  
 8: **Compute (Optional):**  $K_i$  coefficients derivatives using Eq. (D.9) and Eq. (D.16)  
 9: **Compute:** Derivatives of  $M^V$  and  $M^L$  using Eqs. (D.18)–(D.21)

**Algorithm 4.** computeAdditionalDerivatives( $T, p, \mathbf{X}, \beta, \mathbf{y}, \mathbf{x}$ )

- 1: **Inputs:**  $T, p, X, \beta, y, x$   
 2: **Get basic derivatives:** CALL `computeTPvariations(T,p,X,beta,x,y)` Using Algorithm 3  
 3: **Compute:** CALL `computeAdditionalPhaseDerivatives(T,p,X,L,x)` Using Algorithm 5  
 4: **Compute:** CALL `computeAdditionalPhaseDerivatives(T,p,X,V,y)` Using Algorithm 5  
 5: **Compute:**  $\left(\frac{\partial E}{\partial T}\right)_{p,X}$  from Eq. (3.21),  $\left(\frac{\partial E}{\partial p}\right)_{T,X}$  from Eq. (3.22),  $\left(\frac{\partial \rho}{\partial T}\right)_{p,X}$  from Eq. (3.19),  $\left(\frac{\partial \rho}{\partial p}\right)_{T,X}$  from Eq. (3.20),  $\left(\frac{\partial p}{\partial T}\right)_{\rho,X}$  from Eq. (D.22),  $\left(\frac{\partial Z}{\partial T}\right)_{p,X}$  from Eq. (D.30),  $\left(\frac{\partial Z}{\partial p}\right)_{T,X}$  from Eq. (D.31),  $\alpha_p$  and  $\kappa_T$  from Eq. (C.8),  $c_p$  from Eq. (3.8),  $c_v$  from Eq. (2.5),  $\gamma = c_p/c_v$ ,  $\kappa_s$  from Eq. (C.9),  $c$  from Eq. (2.4)

**Algorithm 5.** computeAdditionalPhaseDerivatives( $T, p, \mathbf{X}, \eta, \zeta$ )

---

1:      **Inputs:**  $T, p, \mathbf{X}, \eta, \zeta$ , All other variables already computed in the phase  $\eta$  using Algorithm 3.  
 2:      **Get basic derivatives from the EoS:** Compute  $(\partial Z^\eta / \partial \zeta_k)_{T,p,\mathbf{x},\zeta_k}$ ,  $(\partial Z^\eta / \partial T)_{p,\mathbf{x},\zeta}$ ,  $(\partial \Delta E^\eta / \partial \zeta_k)_{T,p,\mathbf{x},\zeta_k}$ ,  $(\partial \Delta E^\eta / \partial T)_{p,\mathbf{x},\zeta}$ ,  $(\partial \Delta E^\eta / \partial p)_{T,\mathbf{x},\zeta}$ ,  
 $(\partial p / \partial \rho^\eta)_{T,\mathbf{x},\zeta}$ ,  $(\partial p / \partial T)_{\rho^\eta, \mathbf{x}, \zeta}$ ,  $(\partial \rho^\eta / \partial \zeta_k)_{T,p,\mathbf{x},\zeta_k}$  Using an EoS model.  
 3:      **Compute:**  $(\partial \rho^\eta / \partial p)_{T,\mathbf{x},\zeta}$  and  $(\partial \rho^\eta / \partial T)_{p,\mathbf{x},\zeta}$  from Eq. (D.27),  $(\partial \rho^\eta / \partial T)_{p,\mathbf{x}}$  using Eq. (D.24),  $(\partial \rho^\eta / \partial p)_{T,\mathbf{x}}$  using Eq. (D.25),  $(\partial Z^\eta / \partial T)_{p,\mathbf{x}}$  using Eq. (D.28),  
 $(\partial Z^\eta / \partial p)_{T,\mathbf{x}}$  using Eq. (D.29),  
 4:      **Compute:**  $c_v^{i,g} = \sum_{j=1}^{N_g} \xi_{v,j}^{i,g} (c_{v,j}^{i,g})$  precomputed using NASA or CHEMKIN polynomials  
 5:      **Fetch from memory:**  $e_k^{ig}$  (precomputed using NASA or CHEMKIN polynomials)  
 6:      **Compute:**  $(\partial E^\eta / \partial \zeta_k)_{T,p,\mathbf{x},\zeta_k}$  from Eq. (D.34),  $(\partial E^\eta / \partial T)_{p,\mathbf{x},\zeta}$  from Eq. (D.35),  $(\partial E^\eta / \partial p)_{T,\mathbf{x},\zeta}$  from Eq. (D.36),  $(\partial E^\eta / \partial T)_{p,\mathbf{x}}$  from Eq. (D.32),  
 $(\partial E^\eta / \partial p)_{T,\mathbf{x}}$  from Eq. (D.33)

---

**Algorithm 6.** computePartialMolarVolume( $T, p, \mathbf{X}, \beta, \mathbf{x}, \mathbf{y}$ )

---

1:      **Inputs:**  $T, p, \mathbf{X}, \beta, \mathbf{x}, \mathbf{y}$   
 2:      **Obtain liquid mixture:** CALL generateVLstructure( $T, p, \mathbf{x}, L$ ) using Algorithm 1  
 3:      **Obtain vapor mixture:** CALL generateVLstructure( $T, p, \mathbf{y}, V$ ) using Algorithm 1  
 4:      **Compute:** CALL computeAdditionalPhaseDerivatives( $T, p, \mathbf{X}, L, \mathbf{x}$ ) Using Algorithm 5  
 5:      **Compute:** CALL computeAdditionalPhaseDerivatives( $T, p, \mathbf{X}, V, \mathbf{y}$ ) Using Algorithm 5  
 6:      **for**  $i = 1, N_s$  **do**  
 7:        **if**  $i == 1$  **then**  
 8:          **Compute:** Assemble matrix  $\mathbf{C}$  through Eq. (3.29) and compute its inverse  $\mathbf{C}^{-1}$   
 9:        **end if**  
 10:       **Compute:** Assemble vector  $\mathbf{b}_N^{(i)}$  through Eq. (3.30)  
 11:       **Compute and store:**  $\chi_N^{(i)}$  by solving Eq. (3.31)  
 12:       **Compute and store:**  $\delta_{ki} - \chi_{N,k}^{(i)}$  using Eq. (E.12)  
 13:       **end for**  
 14:       **Compute:**  $(\partial \bar{V}^V / \partial N_k^V)_{T,p,N_k^V}$  and  $(\partial \bar{V}^L / \partial N_k^L)_{T,p,N_k^L}$  using Eq. (E.6) and Eq. (E.7) for each  $k$   
 15:       **Compute:**  $(\partial \bar{V}^V / \partial N_i)_{T,p,N_i}$  and  $(\partial \bar{V}^L / \partial N_i)_{T,p,N_i}$  using Eq. (3.27) for each  $i$   
 16:       **Compute:**  $V_i$  using Eq. (3.23) for each  $i$

---

**Algorithm 7.** computePartialMolarEnthalpy( $T, p, \mathbf{X}, \beta, \mathbf{x}, \mathbf{y}$ )

---

1:      **Inputs:**  $T, p, \mathbf{X}, \beta, \mathbf{x}, \mathbf{y}$   
 2:      **Compute:** CALL computePartialMolarVolume( $T, p, \mathbf{X}, \beta, \mathbf{x}, \mathbf{y}$ ) using Algorithm 6  
 3:      **Compute:** Using  $\chi_N^{(i)}$ , compute  $(\partial \bar{E}^V / \partial N_i)_{T,p,N_i}$  and  $(\partial \bar{E}^L / \partial N_i)_{T,p,N_i}$  from Eqs. (E.13)–(E.14)  
 4:      **Compute:** Partial molar enthalpy  $h_i$  using Eq. (3.32)

---

**References**

- [1] P. Aursand, M. Hammer, S. Munkejord, O. Wilhelmsen, Pipeline transport of co2 mixtures: models for transient simulation, *Int. J. Greenh. Gas Control* 15 (2013) 174–185.
- [2] S. Blanco, C. Rivas, R. Bravo, J. Fernandez, M. Artal, I. Velasco, Discussion of the influence of co and ch4 in co2 transport, injection, and storage for ccs technology, *Environ. Sci. Technol.* 48 (2014) 10984–10992.
- [3] H. Li, Thermodynamic Properties of CO2 Mixtures and Their Applications in Advanced Power Cycles with CO2 Capture Processes, Ph.D. Thesis, Royal Institute of Technology, 2008.
- [4] G. Skauen, K. Kolsaker, H. Walnum, O. Wilhelmsen, A flexible and robust modelling framework for multi-stream heat exchangers, *Comput. Chem. Eng.* 49 (2013) 95–104.
- [5] G. Hobold, A. da Silva, A generalized multifluid optimal pressure for heat exchangers operating with supercritical fluid, *Numer. Heat Transf.* 72 (2017) 345–354.
- [6] A. Shojaeian, H. Fatoorehchi, Modeling solubility of refrigerants in ionic liquids using peng robinson-two state equation of state, *Fluid Phase Equilib.* 486 (2019) 80–90.
- [7] M. Pizzarelli, F. Nasuti, R. Paciorri, M. Onofri, Numerical analysis of three-dimensional flow of supercritical fluid in cooling channels, *AIAA J.* 47 (2009) 2534–2543.
- [8] O. Wilhelmsen, G. Skauen, M. Hammer, P. Wahl, J. Morud, Time efficient solution of phase equilibria in dynamic and distributed systems with differential algebraic equation solvers, *Ind. Eng. Chem. Res.* 52 (2013) 2130–2140.
- [9] B.A. Buffett, The thermal state of earth's core, *Science* 299 (2003) 1675–1677.
- [10] W. Thompson, J. Zollweg, D. Gabis, Vapor-liquid equilibrium thermodynamics of n2+ ch4: model and titan applications, *Icarus* 97 (1992) 187–199.
- [11] R. Miller, K. Harstad, J. Bellan, Direct numerical simulations of supercritical fluid mixing layers applied to heptane-nitrogen, *J. Fluid Mech.* 436 (2001) 1–39.
- [12] H. Meng, V. Yang, A unified treatment of general fluid thermodynamics and its application to a preconditioning scheme, *J. Comput. Phys.* 189 (2003) 277–304.
- [13] G. Lacaze, A. Misdariis, A. Ruiz, J. Oefelein, Analysis of high-pressure diesel fuel injection processes using les with real-fluid thermodynamics and transport, *Proc. Combust. Inst.* 35 (2015) 1603–1611.
- [14] T. Schmitt, Y. Méry, M. Boileau, S. Candel, Large-eddy simulation of oxygen/methane flames under transcritical conditions, *Proc. Combust. Inst.* 33 (2011) 1383–1390.
- [15] A. Urbano, L. Selle, G. Staffelbach, B. Cuenot, T. Schmitt, S. Ducruix, S. Candel, Exploration of combustion instability triggering using large eddy simulation of a multiple injector liquid rocket engine, *Combust. Flame* 169 (2016) 129–140.
- [16] P. Yi, S. Yang, C. Habchi, R. Lugo, A multicomponent real-fluid fully compressible four-equation model for two-phase flow with phase change, *Phys. Fluids* 31 (2019) 026102.
- [17] P. Tudisco, S. Menon, Numerical Investigations of Phase-Separation During Multi-Component Mixing at Super-Critical Conditions, 2019, <http://dx.doi.org/10.1007/s10494-019-00101-4>.
- [18] P. Tudisco, R. Ranjan, S. Menon, S. Jaensch, W. Polifke, Application of the time-domain impedance boundary condition to large-eddy simulation of combustion instability in a shear-coaxial high pressure combustor, *Flow Turbul. Combust.* 99 (2017) 185–207.
- [19] P. Tudisco, R. Ranjan, S. Menon, Simulation of transverse combustion instability in a multi-injector combustor using the time-domain impedance boundary conditions, *Flow Turbul. Combust.* 101 (2018) 55–76.
- [20] D. Nicita, P. Khalid, D. Broseta, Calculation of isentropic compressibility and sound velocity in two-phase fluids, *Fluid Phase Equilib.* 291 (2010) 95–102.
- [21] K. Denbigh, The Principles of Chemical Equilibrium: With Applications in Chemistry and Chemical Engineering, Camb. Univ. Press, 1981.
- [22] J. Elliott, C. Lira, Introductory Chemical Engineering Thermodynamics, vol. 184, Prentice Hall, PTR Upper Saddle River, NJ, 1999.
- [23] D. Banuti, The latent heat of supercritical fluids, *Period. Polytech. Chem. Eng.* 63 (2019) 270–275.
- [24] B. Chehroudi, Recent experimental efforts on high-pressure supercritical injection for liquid rockets and their implications, *Int. J. Aerosp. Eng.* 2012 (2012).
- [25] W. Mayer, J. Smith, Fundamentals of supercritical mixing and combustion of cryogenic propellants, liquid rocket thrust chambers: aspects of modeling, *Anal. Des.* 200 (2004).
- [26] W. Mayer, J. Telaar, R. Branam, G. Schneider, J. Hussong, Raman measurements of cryogenic injection at supercritical pressure, *Heat Mass Transf.* 39 (2003) 709–719.

- [27] W. Mayer, A.H. Schik, B. Vielle, C. Chauveau, I. Gökalp, D. Talley, R. Woodward, Atomization and breakup of cryogenic propellants under high-pressure subcritical and supercritical conditions, *J. Propuls. Power* 14 (1998) 835–842.
- [28] B. Chehroudi, D. Talley, E. Coy, Visual characteristics and initial growth rates of round cryogenic jets at subcritical and supercritical pressures, *Phys. Fluids* 14 (2002) 850–861.
- [29] M. Oschwald, A. Schik, M. Klar, W. Mayer, Investigation of coaxial ln2/gh2-injection at supercritical pressure by spontaneous raman scattering, *AIAA* (1999) 1999–2887.
- [30] M. Oschwald, J. Smith, R. Branam, J. Hussong, A. Schik, B. Chehroudi, D. Talley, Injection of fluids into supercritical environments, *Combust. Sci. Technol.* 178 (2006) 49–100.
- [31] M. Habiballah, M. Orain, F. Grisch, L. Vingert, P. Gicquel, Experimental studies of high-pressure cryogenic flames on the mascotte facility, *Combust. Sci. Technol.* 178 (2006) 101–128.
- [32] K.-C. Lin, S. Cox-Stouffer, T. Jackson, Structures and phase transition processes of supercritical methane/ethylene mixtures injected into a subcritical environment, *Combust. Sci. Technol.* 178 (2006) 129–160.
- [33] S. Candel, M. Juniper, G. Singla, P. Scouflaire, C. Rolon, Structure and dynamics of cryogenic flames at supercritical pressure, *Combust. Sci. Technol.* 178 (2006) 161–192.
- [34] A. Roy, C. Segal, Experimental study of fluid jet mixing at supercritical conditions, *J. Propul. Power* 26 (2010) 1205.
- [35] C. Segal, S. Polikhov, Subcritical to supercritical mixing, *Phys. Fluids* 20 (2008) 052101.
- [36] A. Roy, C. Joly, C. Segal, Disintegrating supercritical jets in a subcritical environment, *J. Fluid Mech.* 717 (2013) 193–202.
- [37] N. Zong, V. Yang, Cryogenic fluid dynamics of pressure swirl injectors at supercritical conditions, *Phys. Fluids* 20 (2008) 056103.
- [38] X. Petit, G. Ribert, G. Lartigue, P. Domingo, Large-eddy simulation of supercritical fluid injection, *J. Supercrit. Fluids* 84 (2013) 61–73.
- [39] X. Petit, G. Ribert, P. Domingo, Framework for real-gas compressible reacting flows with tabulated thermochemistry, *J. Supercrit. Fluids* 101 (2015) 1–16.
- [40] M. Masquelet, S. Menon, Y. Jin, R. Friedrich, Simulation of unsteady combustion in a LOX-GH2 fueled rocket engine, *Aerospace Sci. Technol.* 13 (2009) 466–474.
- [41] N. Guezenne, M. Masquelet, S. Menon, Large Eddy Simulation of Flame-Turbulence Interactions in a LOX-CH4 Shear Coaxial Injector, 2012.
- [42] G. Lacaze, J. Oefelein, Modeling of High Density Gradient Flows at Supercritical Pressures, 2013.
- [43] H. Müller, C. Niedermeier, J. Mattheis, M. Pfitzner, S. Hickel, Large-eddy simulation of nitrogen injection at trans-and supercritical conditions, *Phys. Fluids* 28 (2016) 015102.
- [44] A. Ruiz, G. Lacaze, J. Oefelein, R. Mari, B. Cuenot, L. Selle, T. Poinsot, Numerical benchmark for high-reynolds-number supercritical flows with large density gradients, *AIAA J.* (2015).
- [45] T. Schmitt, L. Selle, A. Ruiz, B. Cuenot, Large-eddy simulation of supercritical-pressure round jets, *AIAA J.* 48 (2010) 2133–2144.
- [46] P. Ma, Y. Lv, M. Ihme, An entropy-stable hybrid scheme for simulations of transcritical real-fluid flows, *J. Comput. Phys.* 340 (2017) 330–357.
- [47] P. Ma, H. Wu, D. Banuti, M. Ihme, On the numerical behavior of diffuse-interface methods for transcritical real-fluids simulations, *Int. J. Multiph. Flow* (2019).
- [48] P. Ma, H. Wu, T. Jaravel, L. Bravo, M. Ihme, Large-eddy simulations of transcritical injection and auto-ignition using diffuse-interface method and finite-rate chemistry, *Proc. Combust. Inst.* 37 (2019) 3303–3310.
- [49] K. Harstad, R. Miller, J. Bellan, Efficient high-pressure state equations, *AIChE J.* 43 (1997) 1605–1610.
- [50] N. Okong'o, J. Bellan, Consistent boundary conditions for multicomponent real gas mixtures based on characteristic waves, *J. Comput. Phys.* 176 (2002) 330–344.
- [51] R. Dahms, J. Oefelein, On the transition between two-phase and single-phase interface dynamics in multicomponent fluids at supercritical pressures, *Phys. Fluids* 25 (2013) 092103.
- [52] R. Dahms, J. Oefelein, Non-equilibrium gas-liquid interface dynamics in high-pressure liquid injection systems, *Proc. Combust. Inst.* 35 (2015) 1587–1594.
- [53] A. Firoozabadi, Thermodynamics and Applications in Hydrocarbon Energy Production, McGraw-Hill Education, New York, 2016.
- [54] L. Qiu, Y. Wang, Q. Jiao, H. Wang, R. Reitz, Development of a thermodynamically consistent, robust and efficient phase equilibrium solver and its validations, *Fuel* 115 (2014) 1–16.
- [55] L. Qiu, R. Reitz, Simulation of supercritical fuel injection with condensation, *Int. J. Heat Mass Transf.* 79 (2014) 1070–1086.
- [56] L. Qiu, R. Reitz, An investigation of thermodynamic states during high-pressure fuel injection using equilibrium thermodynamics, *Int. J. Multiph. Flow* 72 (2015) 24–38.
- [57] J. Edwards, R. Franklin, M.-S. Liou, Low-diffusion flux-splitting methods for real fluid flows with phase transitions, *AIAA J.* 38 (2000) 1624–1633.
- [58] A. Star, J. Edwards, K.-C. Lin, S. Cox-Stouffer, T. Jackson, Numerical simulation of injection of supercritical ethylene into nitrogen, *J. Propuls. Power* 22 (2006) 809–819.
- [59] J. Mattheis, S. Hickel, Multi-component vapor-liquid equilibrium model for LES of high-pressure fuel injection and application to ecn spray a, *Int. J. Multiph. Flow* 99 (2018) 294–311.
- [60] C. Traxinger, H. Müller, M. Pfitzner, S. Baab, G. Lamanna, B. Weigand, J. Mattheis, C. Stemmer, N.A. Adams, S. Hickel, Experimental and Numerical Investigation of Phase Separation Due to Multi-Component Mixing at High-Pressure conditions, 2017 arXiv:1706.03923.
- [61] M. Michelsen, The isothermal flash problem. Part I. Stability, *Fluid Phase Equilib.* 9 (1982) 1–19.
- [62] M. Michelsen, The isothermal flash problem. Part II. Phase-split calculation, *Fluid Phase Equilib.* 9 (1982) 21–40.
- [63] B.E. Poling, J. Prausnitz, J.P. O'Connell, The Properties of Gases and Liquids, vol. 5, McGraw-hill, New York, 2001.
- [64] D. Niclita, S. Gomez, E. Luna, Multiphase equilibria calculation by direct minimization of gibbs free energy with a global optimization method, *Comput. Chem. Eng.* 26 (2002) 1703–1724.
- [65] T. Jindrová, J. Mikyška, General algorithm for multiphase equilibria calculation at given volume, temperature, and moles, *Fluid Phase Equilib.* 393 (2015) 7–25.
- [66] T. Smejkal, J. Mikyška, Phase stability testing and phase equilibrium calculation at specified internal energy, volume, and moles, *Fluid Phase Equilib.* 431 (2017) 82–96.
- [67] M. Fathi, S. Hickel, Rapid Multi-Component Phase-Split Calculations Using Volume Functions and Reduction Methods, 2020 (arXiv preprint) arXiv:2001.06285.
- [68] C. Traxinger, M. Banholzer, M. Pfitzner, Real-gas effects and phase separation in underexpanded jets at engine-relevant conditions, *AIAA 2018-1815* (2018).
- [69] C. Rodriguez, H. Rokni, P. Koukouvinis, A. Gupta, M. Gavaises, Complex multicomponent real-fluid thermodynamic model for high-pressure diesel fuel injection, *Fuel* 257 (2019) 115888.
- [70] M. Castier, Thermodynamic speed of sound in multiphase systems, *Fluid Phase Equilib.* 306 (2011) 204–211.
- [71] B. McBride, M. Zehe, S. Gordon, Nasa Glenn Coefficients for Calculating Thermodynamic Properties of Individual Species, 2002.
- [72] R. Kee, F. Rupley, J. Miller, The chemkin thermodynamic data base, From Web (1990).
- [73] L. Sciacovelli, J. Bellan, The influence of the chemical composition representation according to the number of species during mixing in high-pressure turbulent flows, *J. Fluid Mech.* 863 (2019) 293–340.
- [74] C. Lu, Z. Jin, H. Li, A two-phase flash algorithm with the consideration of capillary pressure at specified mole numbers, volume and temperature, *Fluid Phase Equilib.* 485 (2019) 67–82.
- [75] D. Peng, D.-Y. Robinson, A new two-constant equation of state, *Ind. Eng. Chem. Fundam.* 15 (1976) 59–64.
- [76] G. Eliosa-Jiménez, G. Silva-Oliver, F. García-Sánchez, A. de Ita de la Torre, High-pressure vapor-liquid equilibria in the nitrogen + n-hexane system, *J. Chem. Eng. Data* 52 (2007) 395–404.
- [77] R. Poston, J. McKetta, Vapor-liquid equilibrium in the n-hexane-nitrogen system, *J. Chem. Eng. Data* 11 (1966) 364–365.
- [78] M. Michelsen, J. Mollerup, Thermodynamic models: Fundamental and Computational Aspects, 2007.
- [79] J. Carrero-Mantilla, M. Llano-Restrepo, Vapor-liquid equilibria of the binary mixtures nitrogen+ methane, nitrogen+ ethane and nitrogen+ carbon dioxide, and the ternary mixture nitrogen+ methane+ ethane from gibbs-ensemble molecular simulation, *Fluid Phase Equilib.* 208 (2003) 155–169.
- [80] O. Wilhelmsen, A. Aasen, G. Skaugen, P. Aursand, A. Austegard, E. Aursand, M. Gjennestad, H. Lund, G. Linga, M. Hammer, Thermodynamic modeling with equations of state: present challenges with established methods, *Ind. Eng. Chem. Res.* 56 (2017) 3503–3515.
- [81] G. Trappehl, H. Knapp, Vapour-liquid equilibria in the ternary mixtures n2-ch4-c2h6 and n2-c2h6-c3h8, *Cryogenics* 27 (1987) 696–716.
- [82] D. Picard, P. Bishnoi, Calculation of the thermodynamic sound velocity in two-phase multicomponent fluids, *Int. J. Multiph. Flow* 13 (1987) 295–308.
- [83] A. Wood, R. Lindsay, A textbook of sound, *Phys. Today* 9 (1956) 37.
- [84] G. Soave, Equilibrium constants from a modified Redlich-Kwong equation of state, *Chem. Eng. Sci.* 27 (1972) 1197–1203.
- [85] A.M. Aboudour, S.A. Mohammad, R.L. Robinson, K.A. Gasem, Volume-translated Peng-Robinson equation of state for liquid densities of diverse binary mixtures, *Fluid Phase Equilib.* 349 (2013) 37–55.
- [86] J. Jernet, A. Jäger, R. Span, Calculation of phase equilibria for multi-component mixtures using highly accurate Helmholtz energy equations of state, *Fluid Phase Equilib.* 375 (2014) 209–218.
- [87] M. Thorade, A. Saadat, Partial derivatives of thermodynamic state properties for dynamic simulation, *Environ. Earth Sci.* 70 (2013) 3497–3503.
- [88] M. Thorade, A. Saadat, HelmholtzMedia-A fluid properties library, in: Proceedings of the 9th International MODELICA Conference, September 3–5, Munich, Germany, 2012.